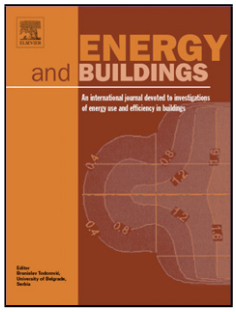

Title: Review on energy savings by solar control techniques and optimal building orientation for the strategic placement of façade shading systems.

Author: <ce:author id="aut0005" author-id="S0378778816320217-c1ddf18268fa5e6d697535ec27f9f5fb"> L.G. Valladares-Rendóna<ce:author id="aut0010" author-id="S0378778816320217-712f74dbf0c299c3210dda7339133156"> Gerd Schmid<ce:author id="aut0015" author-id="S0378778816320217-e1629ac67d0934ed4443c0816f8b3dcd"> Shang-Lien Lo

PII: S0378-7788(16)32021-7
DOI: http://dx.doi.org/doi:10.1016/j.enbuild.2016.12.073
Reference: ENB 7252

To appear in: *ENB*

Received date: 6-7-2016
Revised date: 4-12-2016
Accepted date: 24-12-2016

Please cite this article as: L.G.Valladares-Rendóna, Gerd Schmid, Shang-Lien Lo, Review on energy savings by solar control techniques and optimal building orientation for the strategic placement of façade shading systems., Energy and Buildings http://dx.doi.org/10.1016/j.enbuild.2016.12.073

Review on energy savings by solar control techniques and optimal building orientation for the strategic placement of façade shading systems.

L.G.Valladares-Rendón [a], Gerd Schmid [b], Shang-Lien Lo [a,*]

[a] *Graduate Institute of Environmental Engineering, National Taiwan University,*
71 Fang-Lan Rd., Taipei 106, Taiwan, ROC.
+886233664406
E-mail address: f98541212@ntu.edu.tw (L.G. Valladares-Rendón)

[b] *Department of Mechanical Engineering, National Taiwan University,*
No. 1, Sec. 4, Roosevelt Road, Taipei 106, Taiwan, ROC. R519
+886223631808
E-mail address: d99522042@ntu.edu.tw (Gerd Schmid)

* Corresponding author:
Graduate Institute of Environmental Engineering, National Taiwan University,
71 Chou-Shan Rd., Taipei 106, Taiwan, ROC. R300-B
Tel.: +886 2 23625373; fax: +886 2 23928821
E-mail address: sllo@ntu.edu.tw (S.-L. Lo).

Highlights

Passive cases with strategies of solar control reduced insolation and energy demands

A simple design with mixed strategies saved 76.57% while a complex design alone 66%

The most suggested solutions are complex FSS and SDs but well-oriented and designed

Optimal azimuth angle is crucial indicator for planning strategic designs placement

Complex designs can be used for the integration of renewable solar cooling system

Abstract

Urban patterns without highly designed buildings increase the urban heat and energy demands. Solar control techniques encompass strategies that, if properly designed and applied, can decrease solar radiation and cooling demands. The aim of this research is to establish and recommend the most effective and balanced solutions to decrease insolation and increase energy savings while balancing daylighting and visibility. Four main classes were reviewed: façade self-shading, shading devices, window-to-wall-ratio and building orientation. The results showed that the cases with such passive strategies effectively lowered the insolation and achieved potential energy savings of 4.64% to 76.57%. The strategies selected for six cases were suitable for subtropical and temperate zones. The most recommended solutions were complex designs of façade self-shadings and shading devices; their strategic placements and accurate designs can further improve their performance. The optimal building orientation is essential for determining optimal façades for the strategic placement of both complex and simple designs. A worldwide guide of azimuth angles was calculated for 59 locations. The results show that 58.62% locations should apply complex designs to the east, 24.13% to the northeast, 12.06% to the west and 5.17% to the southeast orientations for solar protection. In tropical and subtropical zones, complex designs can be integrated with renewable technologies.

Keywords: sustainable cities development, passive cooling strategies, solar control techniques, potential energy savings, façade shading systems, optimal azimuth angles.

Nomenclature	
A	Surface area (m^2)
ALT	Solar altitude
AZM	Solar azimuth
d	Distance (m)

DD	Device depth (m)
DHD	Depth horizontal device (m)
DVD	Depth vertical device (m)
E	Total energy gained (kW)
GWA	Gross wall area (m^2)
h	Height (m)
HSA	Horizontal shadow angle
HVD	Height vertical device (m)
HW	Window height (m)
i	Incidence angle
L°	Latitude on the north hemisphere
M	Monthly mean daily global radiation
NGA	Glazing area (m^2)
OSN	Surface orientation normal
VSA	Vertical shadow angle
$\tilde{V}$	Angle from horizontal floor to wall
WHD	Width horizontal device (m)
WW	Width of window (m)
X°	Summer angle measured from window sill to sun's altitude
Y°	Winter angle measured from window frame head to sun's altitude
$\hat{Z}$	Angle between zenith and sun's altitude
Greek symbols	
θ_z	Zenith angle
$\omega_{1,2}$	Sunrise and sunset the hour angles
Acronyms	
Af	Tropical rainforest no summer no winter
Aw	Tropical savanna summer wet season winter dry season
ASHRAE	American Society of Heating, Refrigerating and Air-Conditioning Engineers
BAR	Building aspect ratio
BO	Building orientation
BSk	Semi-arid steppe cold
BWh	Arid desert hot
Cfa	Temperate no dry season hot summer
Csa	Mediterranean dry summer hot summer
Cwa	Temperate dry winter hot summer
Dfa	Continental no dry season hot summer
Dfc	Continental subarctic no dry season cold summer
DHG	Dissipate heat group
Dsa	Continental dry summer hot summer
Dsd	Continental subarctic dry summer very cold winter
Dwa	Continental dry winter hot summer
E	East
EDR	Energy demand reductions
FSS	Façade self-shading
HVAC	Heating, ventilation air conditioning
MHG	Modulate heat group
N	North
NECB	National Energy Code for Buildings
OBO	Optimal building orientation
OBOSP	Optimal building orientation for solar protection
OBOSC	Optimal building orientation for solar collection
PCS	Passive cooling strategies
PES	Potential energy savings
PHG	Preventive heat group
RES	Renewable energy sources
RSCT	Renewable solar cooling technologies
S	South

SCT	Solar control techniques
SDs	Shading devices
SUBT	Subtropical zone
TEMP	Temperate zone
TROP	Tropical zone
W	West
WWR	Window-to-wall-ratio

1. Introduction

Strong economic growth and fast urban development have generated urban patterns with an absence of highly designed buildings, which thus increases the urban heat and energy demands. Of the total global energy consumption in the building sector in 2010, 20% was consumed by China, 19% by the United States, 15% by the OECD countries, 6% by Russia and 40% by other countries [1]. The worldwide building energy consumption is expected to increase at an average rate of 1.5% per year from 2012 to 2040 [2]. Most of this energy is derived for space cooling, space heating, lighting and appliances. Energy demands for space heating in cold climates and space cooling in hot climates are among the world's biggest concerns. However, the adaptation of renewable technologies in European countries is expected to reduce energy use for heating and cooling by up to 70% by 2050 [3]. Additionally, in Asian countries, it is estimated that by 2050 the average cooling energy in residential and commercial buildings will increase by up to 750% and 275%, respectively [4]. One factor increasing the energy demands is the impact of direct and diffuse solar radiation on urban centres, which raises the surface and air temperatures. The resulting reservoir of heat waves during the day and night, known as the urban heat island phenomenon, can produce changes in the local, regional and global climate. This rise in air temperatures lowers heating demands on the one hand but enlarges cooling demands on the other [5]. Thus, the amount of incident solar radiation (insolation) reaching the buildings' surfaces plays an important role in regulating the energy demands and global climate. The outcome of the incident, reflected, absorbed and transmitted energy in a building might depend on the geographical location, the local climate, the urban context, its design, thermal mass and materials. A study conducted by Santamouris [4] stated that poorly designed buildings are more likely to

absorb solar radiation, resulting in quick heat gains that increase the cooling energy demands. These heat gains can be difficult to remove and might need additional natural, renewable or mechanical systems [6]. By contrast, highly designed buildings, apart from controlling the impacts of solar radiation, can slow down this heat transfer, thus reducing the internal energy demands, which results in energy savings for air conditioning systems (HVAC). **Fig. 1** shows a diagram of insolation and energy savings in buildings with and without a passive design [7].

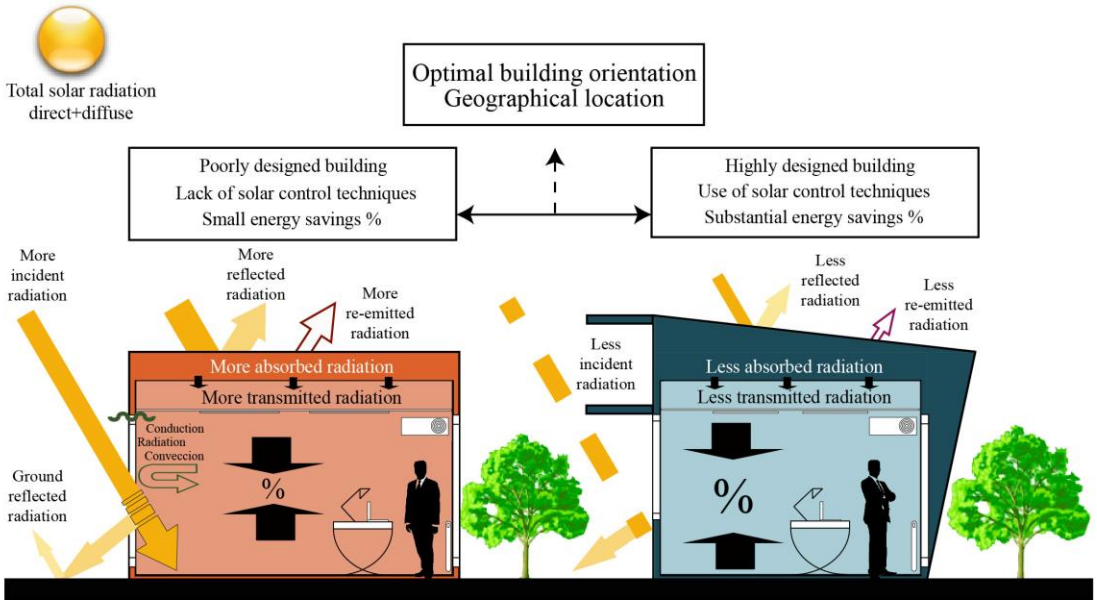

Fig. 1 Schematic sections in 2D view of insolation and energy savings in buildings with and without a passive design [7].

In an effort to reduce energy demands in residential, commercial and industrial buildings, several energy efficiency policies, programmes, codes, ratings and standards have emerged in the last decades [8]. Other building regulations have been developed and enforced by governments, especially in the USA [9], Europe [10] and China [11]. Most of them agreed that the key elements for developing sustainable cities are the adaptation of passive building design, energy-efficient materials and technologies, which should be considered before any mechanical system. These criteria are crucial to improve the energy performance in an environmentally

responsible manner. Various key elements for developing sustainable cities are illustrated in **Fig. 2** [12][13].

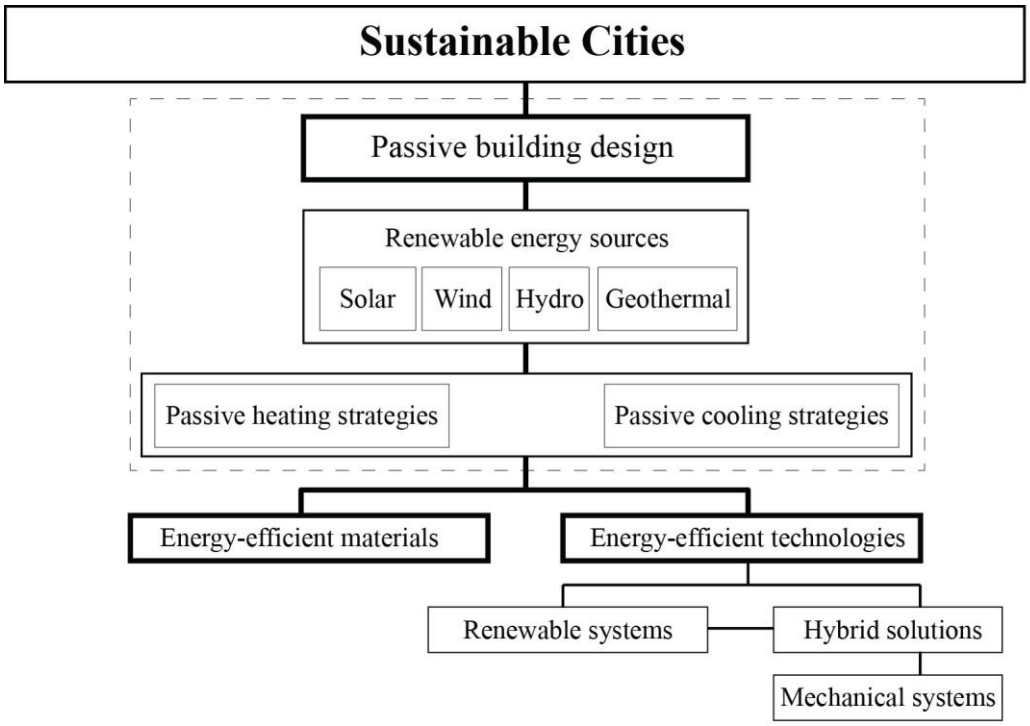

Fig. 2 Key elements for developing sustainable cities [12][13].

Passive building design is a fundamental decision during the planning process because it can take advantage of the natural and renewable energy sources (RES) occurring at the building's site to maximise comfort and minimise energy demands [14]. This approach can trigger a positive chain reaction leading to downsizing mechanical equipment, reducing cost of electricity bills, mitigating environmental impacts and enhancing thermal comfort and health [15][16]. Passive cooling strategies (PCS) are sustainable design concepts which use zero or low energy input to keep indoor spaces cooled while capitalising on energy savings [17]. A wide diversity of PCS can be classified into three groups that prevent, modulate or dissipate heat [18]. The preventive heat group (PHG) seeks to eliminate the possibility of heat gains by blocking the sun’s radiation from entering the building. The strategies of the modulate heat group (MHG) attempt to modify the heat gained in the space. Usually,

this heat is stored during the day and slowly released during the night. The strategies of the dissipate heat group (DHG) aim to remove heat from the building using on-site natural cooling [19]. Most of the PCS within these three groups require no energy input other than RES [18]; however, some passive strategies within the DHG might need a low energy input [17]. **Fig. 3** presents an overview of the PCS to prevent, modulate and dissipate heat [18].

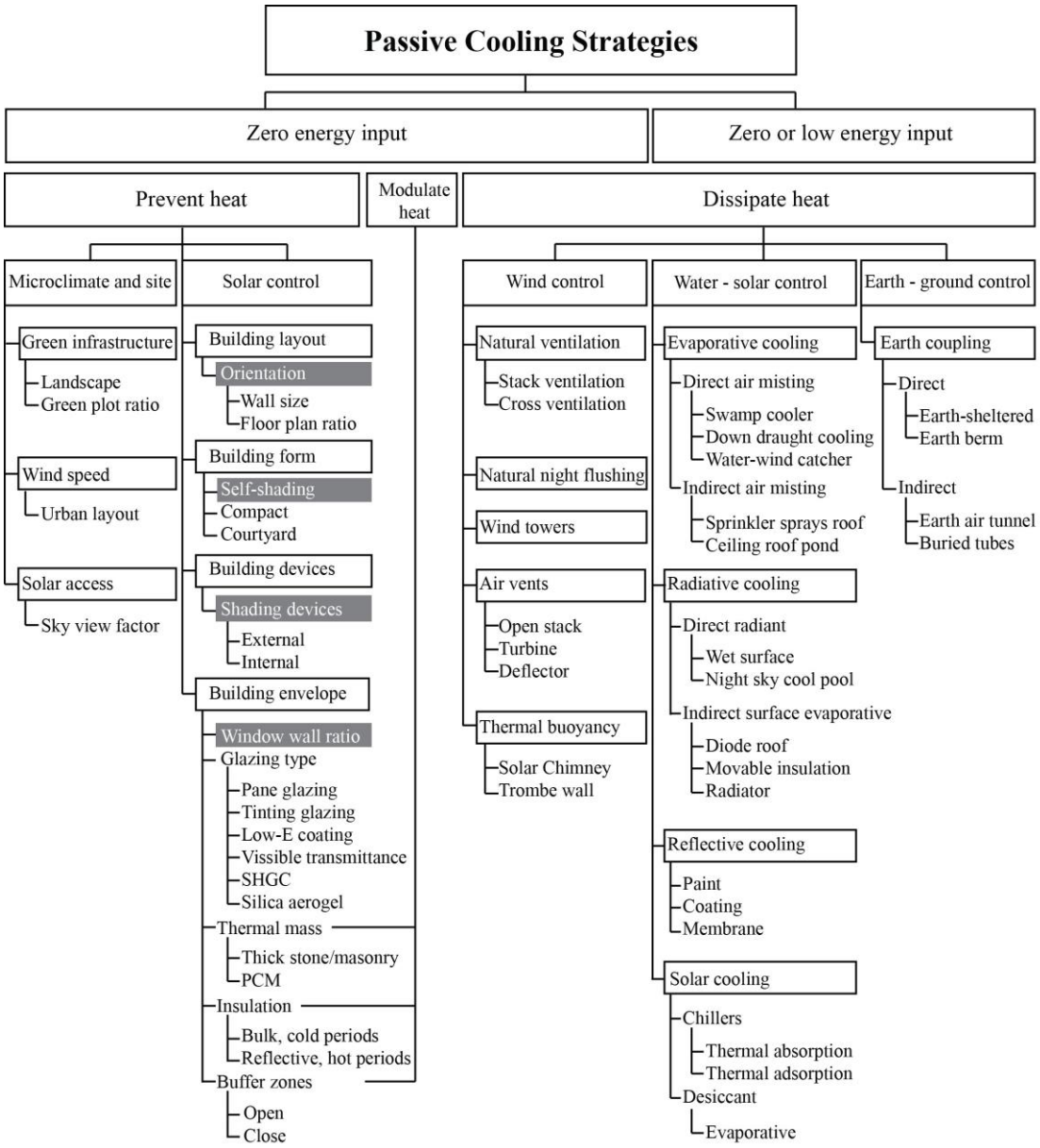

Fig. 3 Overview of PCS to prevent, modulate and dissipate heat [18].

The energy performances of the PCS within the PHG, MHG and DHG have been broadly studied [18]. The PHG comprises two main techniques: the microclimate-site and solar control. Each presents several features that are able to mitigate the urban heat island and enhance the building's energy-efficiency. The main features listed within the microclimate and site technique are green infrastructure, wind speed [19] and solar access [20], whereas the features within the solar control technique are building layout, form, devices and envelope. Each of these features contains several classes of passive strategies that could prevent the entry of insolation into the space. Some of these classes of passive strategies, such as orientation, shape, shading, insulation, and their incidences on total energy demand have been examined by Pacheco et al. [2]. They concluded that orientation, shape and shading strategies are effective at blocking insolation and have a great effect on final energy demand. Three other classes of passive strategies within the MHG that can enhance the envelope's proper operation and achieve energy savings are thermal mass, insulation and vaulted roofs, as discussed by Sadineni et al. [21]. The authors found that passive energy efficiency strategies are very sensitive to meteorological conditions and that thermal mass is more effective in places with extreme temperatures during the day and night. In order to economically reduce the building cooling demands and downsize the HVAC system, Kamal [22] examined and discussed several techniques within the DHG, such as wind, water-solar and earth-ground, and concluded that to achieve desirable reductions in energy demands, it is essential to understand the micro-climate around the building. One of the features within this group, which has been widely used to lower heat transfer into the building and reduce energy loads, is reflective cooling. Al-Obandi et al. [23] demonstrated the reduction of outdoor and indoor heat by applying reflective paint to a building's surfaces; this strategy is particularly

feasible in tropical climates. The advanced solar cooling technologies, which use renewable solar energy as a source for cooling were studied by Gagliano et al. [24]. The authors stated that this solar air conditioning is a viable solution in warm climates from an economical and environmental viewpoint.

Among the PCS are two interesting bioclimatic approaches for controlling insolation for cooling modern buildings [25]: (1) solar control techniques (SCT) that are designed for solar protection and (2) renewable solar cooling technologies (RSCT) that are designed for solar collection, but for cooling purposes. However, their thermal, daylighting and visual performance might be subject to the renewable sources available at the site, the strategy selected and their appropriate orientations [26]. SCT encompass a large number of strategies that could be highly designed to decrease the impacts of solar radiation on the building envelope and on the interior space to reduce cooling energy demands. The four main classes which can decrease insolation, increase shading and reduce energy demands are façade self-shading (FSS), shading devices (SDs), window-to-wall-ratio (WWR) and building orientation (BO). However, the inappropriate selection and application of these strategies can compromise the daylighting and visibility comfort [27].

The aim of this research is to recommend the most effective passive solutions to decrease insolation and increase energy savings for cooling systems, while balancing daylighting and visibility. It is essential to ensure the strategic placement and accurate design of the passive solutions from the beginning of a project to achieve desirable results. Therefore, this study additionally provides a worldwide guide of azimuth angles, to determine optimal façades for the strategic placement of effective and balanced designs. The suggestions made in this study will be useful for developing more effective and balanced designs worldwide. In the second section of this

manuscript, several cases within the FSS, SDs, WWR and BO classes are reviewed in terms of solar radiation and energy demands and the passive cases are compared to the base cases to obtain the energy demand reductions (EDR) and the potential energy savings (PES). Consecutively, the third section presents the results, which were analysed, discussed and evaluated. The EDR and PES are then summarised to obtain the percentage range of the PES achieved by the passive cases **Table 2** and the PES achieved by each passive case is classified by location and climate to reveal suitability of the selected passive strategies **Fig. 9**. Then, the PES achieved by each passive case are analysed by performance to identify the more effective combinations of passive strategies **Fig. 10**. Afterwards, each strategy type is classified by its PES and categorised by parameters to find which design parameter strongly influences the PES **Table 3**. Additionally, all of the strategy types are evaluated in terms of insolation, daylighting, visibility and PES to recommend designs and parameters for developing more effective and balanced solutions. In the fourth section, a worldwide guide of azimuth angles is calculated (**Table 4**) and classified by orientation (**Fig. 12, 13**) to determine optimal façades for the strategic placement of effective and balanced designs.

2. Passive cooling strategies of solar control to decrease insolation and energy demands

In this second section of the manuscript, several cases within the FSS, SDs, WWR and BO classes are reviewed in terms of solar radiation and energy demands. The passive cases (with passive strategies) against the base cases (without passive strategies) are compared to obtain the EDR and the PES.

2.1 Façade self-shading

FSS is an aesthetic and functional skin of a building. The target of FSS is to lower the insolation on the opaque and glazing elements of the building during a required period. Decreased heat gains on the building envelope can lower the energy demands [28][29]. There are simple designs which are effective in blocking insolation during noon time and other more complex designs that are able to protect from severe insolation between early morning and late afternoon. Different types of self-shading façades are illustrated in **Fig. 4** [30].

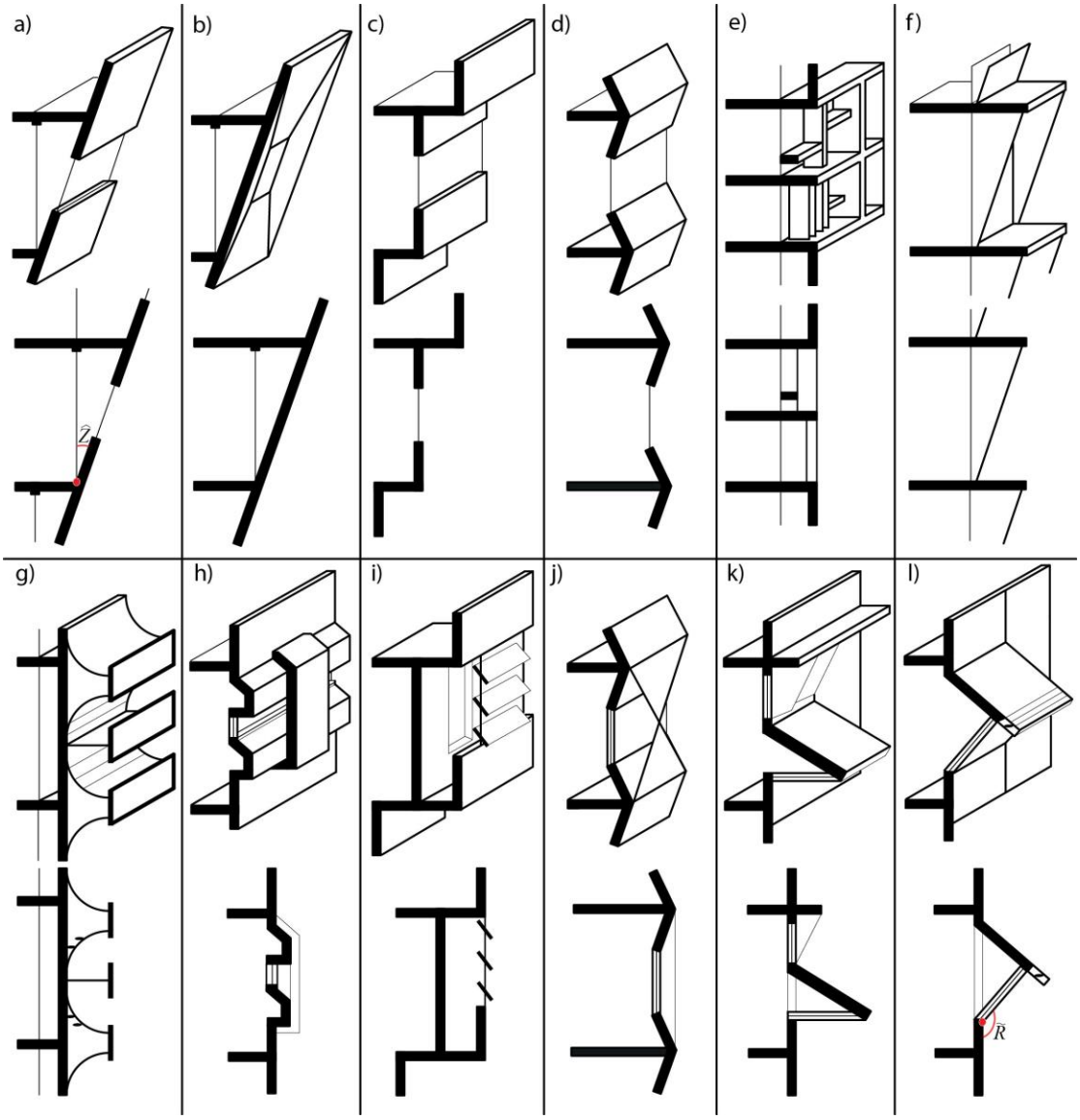

Fig. 4 Schematic sections in 2D and 3D views of façade self-shading, simple designs a) to f) and complex designs g) to l): a) Tilted flat with rectangular opening, b) Tilted with texture and square opening, c) Step with rectangular opening, d) Waterfall with rectangular opening, e) Filled eggcrate with mini enclosure and full glazing, f) Zig-zag balconies with full glazing, g) Horizontal outer panels with louvres and full glazing, h) Waves with horizontal opening, i) Step with tilted panels and vertical opening, j) Waterfall with triangle panels and rectangular opening, k) Skylight cantilever with tilted shark panels, l) Skylight cantilever with tilted louvre [30].

The formula to ensure that a certain point on the façade is under the shade of the roof contour during a required period is given by Eq. (1) [30]:

$$h = d / \tan \hat{Z} \quad (1)$$

Where, h is the height from the certain point in the façade to be under shade perpendicular to a point in the roof mesh, d is the distance from a point in the roof mesh towards the roof's contour and $\hat{Z}$ is a wall angle between the zenith and the sun's altitude [30].

The effectiveness of FSS, which is designed to decrease insolation and energy demands was analysed in different locations and climates, including Israel [30], Greece [31] and China [32]. In a prismatic building, by increasing the inclination degree of the façades and combining it with other passive strategies, the insolation across the building envelope and the energy demands dropped. An office space in the upper part of a building in Jerusalem, Israel demonstrated that by adapting to its orthogonal walls, a second inclined wall with double glazing and internal blinds not only decreased the insolation and energy demands, but also enhanced the shading at pedestrian levels. This system in a Csa climate improved the building energy performance when the $\hat{Z}$ angle on the S façade was 31°, on the E and W façades 34° and without inclination on the N façade. The office W façade with a $\hat{Z}$ angle of 34° (see **Fig. 4a**) was able to lower its energy consumption by 0.64 kWh/m^2/y (43%) [30].

It was further emphasised that FSS can save more energy than using vertical façades with low-emissivity windows. Similarly, in a Csa climate, such as that found in Athens, Greece, a study investigated the air flow and energy performance in a semi-prismatic building. Zerefos et al. [31] found that during summer the inclined roofs and walls effectively lowered the insolation impacts and energy demands. The thermal zones of an orthogonal building were higher than those in the semi-prismatic building. The NW zone of the semi-prismatic building, which had a tilted roof and a W façade with a $\hat{Z}$ angle of 7°, achieved a reduction in the annual cooling load of about 40.8 kWh/y (4.64%). A slight inclination on the building façades helped to slow down the heat gains, especially during the summer periods. In another prismatic building, Chan and Chow [32] evaluated the repercussion of FSS on the annual cooling and heating loads in different climates, such as those found in Shanghai, Beijing and Hong Kong. They found that the energy performance of the upside down pyramid in different climates was contradictory. In a building floor with external walls at $\hat{Z}$ angles of 40°, the heating demands were increased in the first two locations; however, in a Cwa climate, such as that found in Hong Kong, the cooling demands were reduced by 7.51 kWh/m^2/y (10.95%). Additionally, by changing the $\hat{Z}$ angle to 50° or 30°, the savings were marginally lower because higher inclinations allow more entrance of reflected radiation emitted from the floor. In an urban context, insolation coming from hard surfaces can likewise influence the energy performance.

2.2 Shading devices

As practical and low maintenance elements, SDs are increasingly used to block insolation impacts. The target of SDs is to enlarge the shading ratio, especially on windows, to keep spaces conditioned, lower energy demands and reduce glare levels near windows. Proper designs prevent overheating during summer whilst allowing

maximum daylight to enter during winter [33][34]. In general, external SDs have a higher performance than internal ones [35] and fixed SDs are economical solutions, as they do not require manual adjustments [36][37]. **Fig. 5** shows the different types of external SDs [33][38][39].

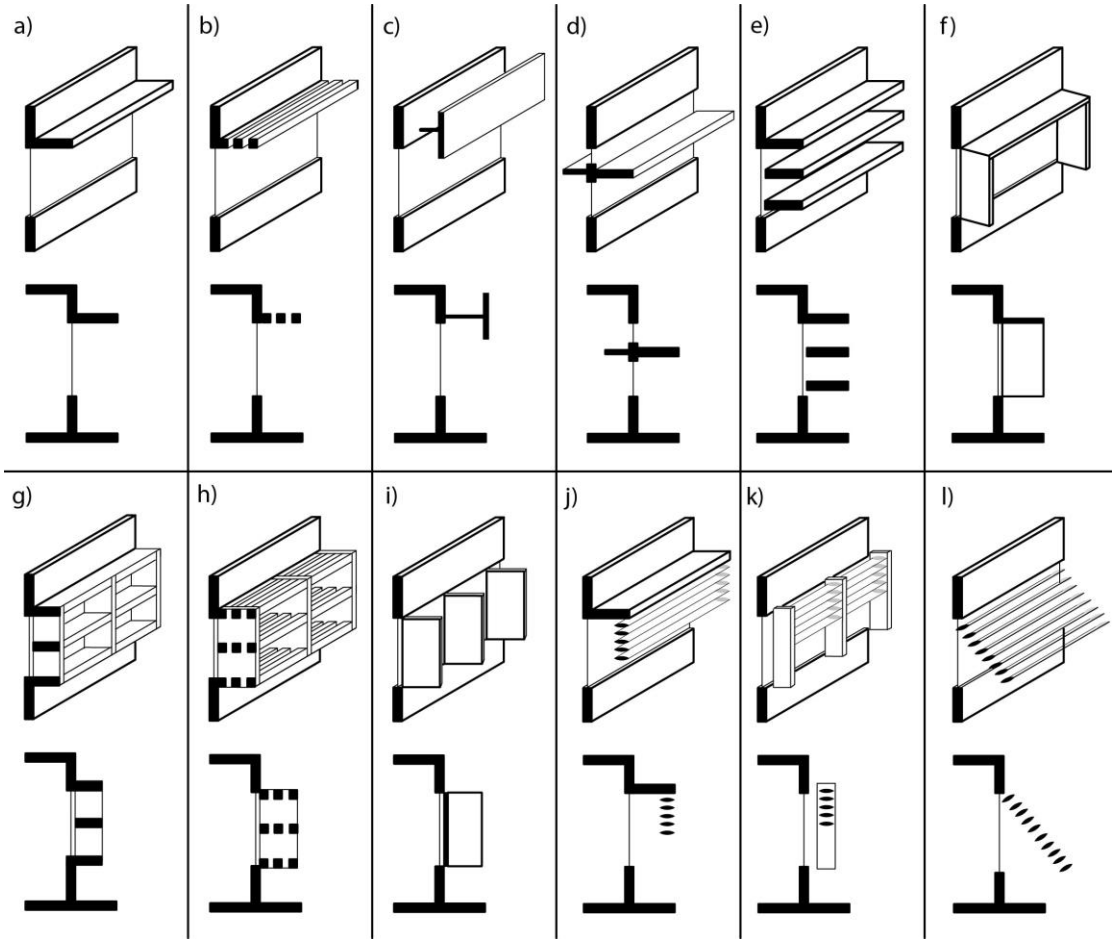

Fig. 5 Schematic sections in 2D and 3D views of external SDs, simple designs a) to f) and complex designs g) to l): a) Horizontal overhang or panel, b) Horizontal louvers or outrigger system, c) Vertical outer panel, d) Horizontal light shelve, e) Horizontal multiple blades or panels, f) Unfilled eggcrate, g) Filled eggcrate with panels, h) Filled eggcrate with horizontal louvre, i) Vertical slanted fins or panels, j) Horizontal panel and vertical louvers, k) Vertical panels and horizontal louvers, l) Cantilever tilted slats [33][38][39].

SDs must be adapted to seasonal solar variations occurring at different locations. To design effective SDs, the sun's position with respect to the surface normal of a vertical plane needs to be known [40]. An illustration of the insolation occurring

during the seasonal variations in the North Hemisphere at latitude 24° is shown in **Fig. 6a** [40].

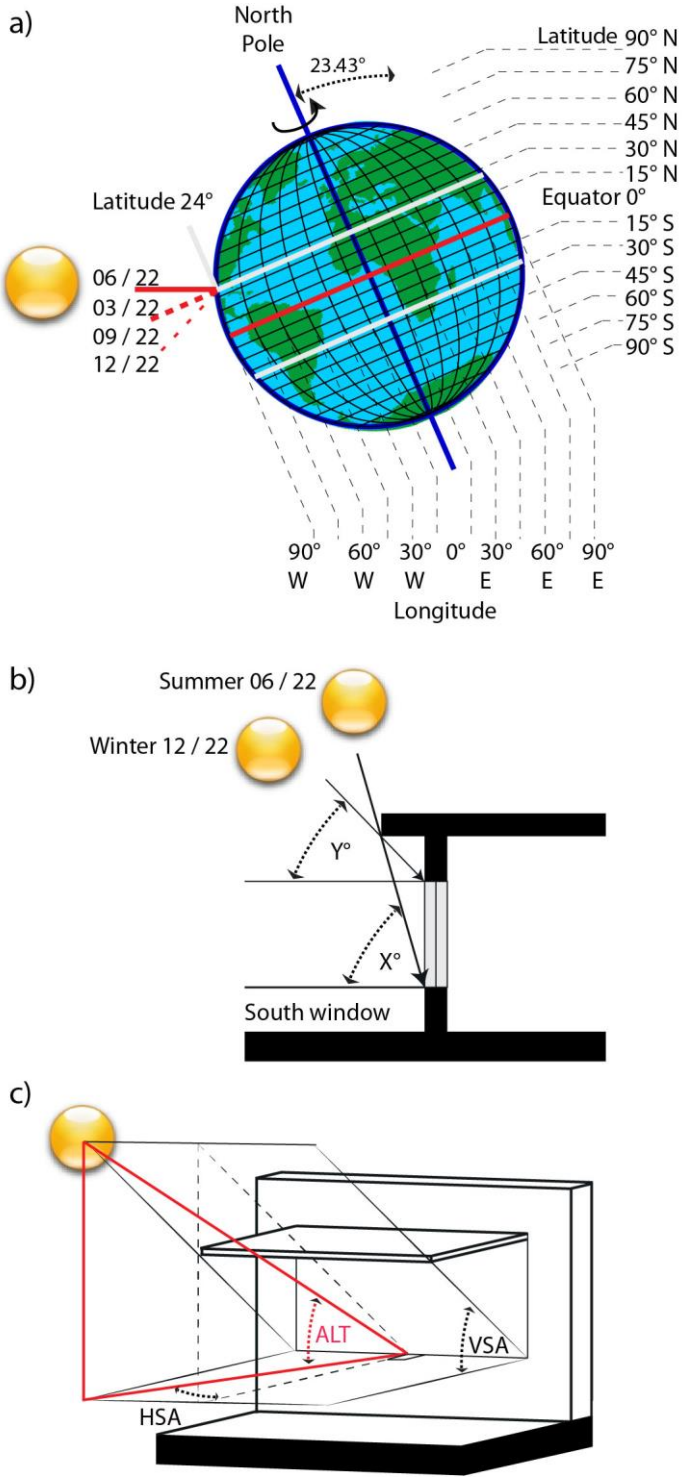

Fig. 6 Schematic elevations in 2D and 3D view: a) insolation occurring during the seasonal variations in the Northern Hemisphere at latitude 24°, b) solar angles for sizing overhangs on S-facing façades during summer and winter and c) solar altitude and shadow angles for sizing shading devices at any

latitude [40][41][43].

A brief guidance of the solar angles for sizing overhangs on S-facing façades in the Northern Hemisphere according to the Earth's latitude is presented in **Table 1** and illustrated in **Fig. 6b** [40][41]**.**

Table 1 Angles for sizing overhangs on S-facing façades of the Northern Hemisphere according the Earth's latitude [40][41].

$L°$	24	25	26	27	28	29	30	31	32	33	34	35	36	37	38	39	40	41	42	43	44	45
$X°$	74	73	72	71	70	69	68	67	65.5	64.5	63.5	62.5	60.5	59.5	59	58.5	58	57	56	55	54	53
$Y°$	46	45	44	43	42	41	40	39	37.5	37.5	35.5	34.5	32.5	31.5	31	30.5	30	29	28	27	26	25

Where, $L°$ represents the Earth's latitude on the Northern Hemisphere, $X°$ the summer angle measured from the window sill to the sun's altitude and $Y°$ the winter angle measured from the window head to the sun's altitude [40][41].

A traditional method for shading windows using SDs consists of first knowing the sun's altitude and azimuth. In a section view, the solar altitude (*ALT*) is the vertical angle from a sun's path or horizontal plane to the sun. From a top view, the solar azimuth (*AZM*) is an angle measured on the sun's path or horizontal plane from the true north clockwise [42]. However, when attempting to accurately shade the glazing areas at any latitude, the horizontal shadow angle (*HSA*) and vertical shadow angle (*VSA*) relative to a window at the current date and time are more important. The *HSA* is the angle between the window surface normal or the orientation that a given surface is facing (*OSN*) and the *AZM* taken over a horizontal plane at the bottom of the window. The *VSA*, which is the angle between the horizontal plane to the solar altitude, is indicated in **Fig. 6c** [43]. The formula to calculate the *HSA* is given by Eq. (2) and the *VSA* by Eq. (3) [43]:

$$HSA = AZM - OSN \tag{2}$$

$$VSA = arctan\,(tan\,ALT\,/\,cos\,HSA) \quad (3)$$

Usually this method is followed by the application of several calculations to determine the shape of the SDs [44]. The depth and the width of a horizontal SDs can be calculated using Eq. (4) and Eq. (5) [44]:

$$DHD = HW/tan\,VSA \quad (4)$$

$$WHD = DD \times tan\,HSA \quad (5)$$

Where, *DHD* is the depth of the horizontal device, *HW* is the window height, *WHD* is the width of the horizontal device and *DD* is the device depth.

The depth and the width of a vertical shading device can be calculated using Eq. (6) and Eq. (7) [45]:

$$DVD = WW/tan\,HSA \quad (6)$$

$$HVD = DD \times tan\,VSA \quad (7)$$

Where, *DVD* is the depth of the vertical device, *WW* is the width of window and *HVD* is the height of the vertical device.

In recent years, computational software has incorporated traditional methods and sun path diagrams to create precise tools for sizing and shaping SDs [46]. The effectiveness of SDs to decrease insolation and reduce energy demands were examined in Taiwan [47], South Korea [48], Singapore [49] and South Korea [50]. The decrease of insolation levels and the increase in energy savings achieved by different horizontal overhangs were analysed in a Cfa climate such as that in Taipei,

Taiwan. Valladares-Rendón and Lo [47] reported that SDs diminished the insolation on the whole building's envelope and at the same time increased the shading ratio on the outside. It was concluded that the use of such devices helps to slow down the heat transfer and reduce the cooling loads. The floor's thermal performance of a bare building was compared with one using SDs. It was found that horizontal overhangs applied together, as single, edge and layer, in a rectangular building was the most effective system and could reduce the annual cooling loads by 16.73 kWh/m^2/y (8.92%). Compared to other SDs, the combined system provided shade to the opaque and glazing elements, preventing overheating on the whole building. In a Dwa climate, such as that in Seoul, South Korea, the cooling loads of several external SDs, distributed in different orientations of a high-rise rectangular building were analysed. The findings indicated that horizontal overhangs were suitable for windows oriented to the S, E and W, though not for those oriented to the N. The proper application of SDs not only equilibrates shading and daylighting, but also improves the energy savings on cooling compared with vertical ones. A single unit on the S side of a building's floor with and without SDs was analysed from May to September. During this period, the S-facing unit with a horizontal overhang was able to reduce the cooling loads by 14.81 kWh/m^2 (19.70%) [48]. Overhangs at the right place diminish unwanted insolation and reduce a large part of the energy intake needed for HVAC systems. In Singapore, which has an Af climate, it was found that the heat accumulation on the building envelope strongly affected the energy consumption. By adding SDs and other glazing types, the heat transmission through the building envelope could be minimised. The low rate of heat transfer passing through the shaded glazing reduced the space cooling loads and the capacity of the HVAC equipment. SDs on rectangular buildings were found to be very effective in reducing

space cooling and performed better than double glazing. The energy performance of a non-shaded rectangular building was compared against a shaded one on the E and W façades. The overhang tilted 30° downward on the W side reduced the annual space cooling loads by 21.20%, which was 7.20% higher than a simple horizontal projection [49]. Tilted projections designed according to local conditions and orientations can effectively extend the time of protection over the envelope elements. In a Dwa climate, such as that in Seoul, South Korea, several SD simulations demonstrated that only certain types of devices can lower insolation without compromising the visibility and thermal performance. Kim et al. [50] emphasised that this balance was controlled by the overhang's depth and slat angle. A unit in a bare rectangular building was compared to one with different types of SDs. The application of a fixed tilted overhang with adjustable slats at 60° (see **Fig. 5(l)**) on the S windows promised annual cooling load reductions of 22.68 kWh/m^2/y (66%). Fixed devices must be carefully designed to fulfil the intended purpose on each façade. Well-designed devices provide a good balance between shading, daylighting and visibility.

2.3 Window-to-wall-ratio

The WWR is the percentage of glazing area to the wall area of a building façade [51]. The target of the WWR is to reduce solar heat gains and improve heating, cooling, daylighting and ventilation. Therefore, the National Energy Code for Buildings (NECB) 2011 and the American Society of Heating, Refrigerating and Air-Conditioning Engineers (ASHRAE 90.1) have incorporated the WWR into its standards for new building construction [52]. The WWR is measured on a scale from 0% to 100% or from factor 0 to 1 for no windows to full windows, respectively. These two extremes usually result in negative effects in terms of energy, daylighting and

visibility. **Fig. 7** illustrates the different WWRs in relation to their daylighting and visibility [53]**.**

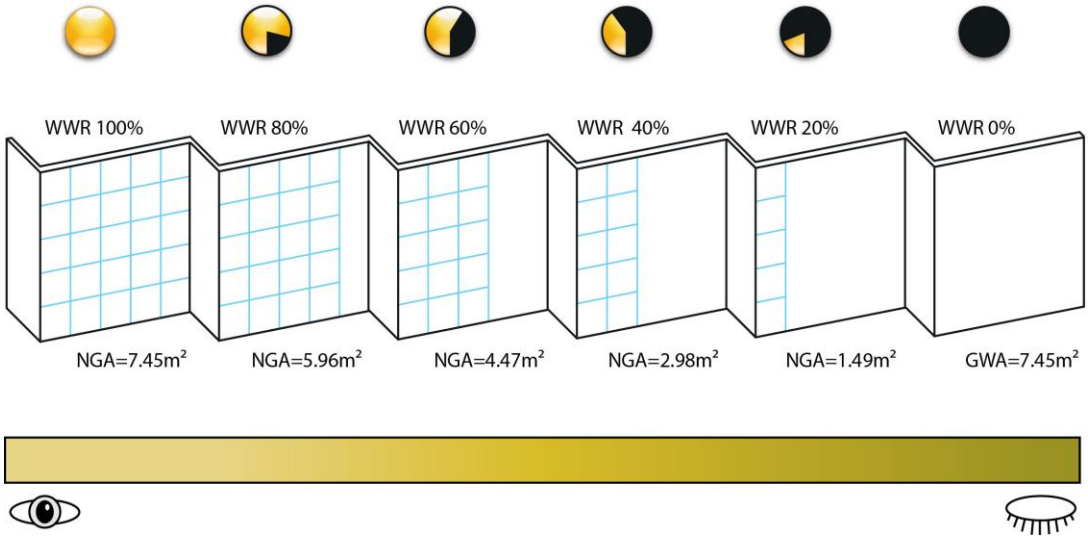

Fig. 7 Schematic 3D view of WWRs in relation to their daylighting and visibility [53]**.**

A common rule of thumb states that to enhance a building's energy performance, the optimal WWR for hot and cold climates should be around 40% or less. A higher WWR up to 90% can be accepted in cold climates, but only if the windows are well insulated, and in hot climates, only if they are well shaded [54]. The formula to calculate the window wall ratio is given by Eq. (8) [54]:

$$WWR = NGA/GWA \tag{8}$$

Where, *NGA* is the net glazing area and *GWA* is the gross wall area [54].

The effectiveness of the WWR designed to decrease insolation and achieve reductions on energy demands were investigated in Turkey [55], China [56], Chile [57] and Norway [58]. A study in five different locations in Turkey examined the WWR, building aspect ratio (BAR), glazing type and insulation required to keep the building's thermal balance. Inanici and Demirbilek [55] found that double glazing and a higher insulation has direct impacts on heating loads. Additionally, when the BAR with fixed WWRs were changed simultaneously, the total energy demands remained

unaffected. However, when the WWR was modified only on the S side, the total loads were strongly affected. The S zones of a square building located in Antalya, Turkey showed that by decreasing the S WWR from 90% to 25% in a Csa climate, the insolation was lowered and the total load was reduced by 36.11 kWh/m^2/y (54.17%). Additional improvements could be achieved by considering windows with low solar heat gain coefficients or additional SDs. In a hotel building in Guiyang, China the impact of different WWRs and the envelope's U-value on the all-year cooling load was examined. It was found that in a Cwa climate, the cooling loads were influenced more by lowering the WWR, rather than by glazing with a low U-value. Additionally, in a square building lowering the S WWR from 70% to 25%, less insolation entered the inside resulting in annual cooling load reductions of 114,429 kWh/y (53.98%) [56]. Notably, at this location, the S WWR had a considerable effect on the building gains and losses. The total annual energy demands in an office building in Santiago, Chile, which considered WWR, SDs, double glazing and night ventilation were estimated. Pino et al. [57] found that a square building in a BSk climate with 100% glazing is not recommended. Nevertheless, the performance of an entire floor with a 20% WWR (see **Fig. 7**), double glazing, additional horizontal overhangs on the N façade and internal blinds on the E and W façades decreased the total annual energy demand by 82.4 kWh/m^2/y (76.57%). Smaller WWRs control the solar radiation penetrating into the indoor space, thus lowering the energy demands; unfortunately, the visibility to the outside can also be restricted. In a Dfc climate, such as that found in Oslo, Norway, several simulations were carried out to determine the optimal WWR, glazing panes and SDs to reduce the net energy demands. The authors found that by comparing the total net energy demands between a single and double S-facing cubicle, the single-person cubicle without shading, but with a 61% WWR and two-pane

glazing, had the worst performance. Whereas, when the WWR of the single-person cubicle was lowered from 61% to 41% with additional four-pane glazing, the total net energy was reduced by 52 kWh/m^2/y (27.95%) [58]. Low WWRs effectively reduce energy demands and insolation impacts, but the effect of the latter is limited. During the early morning or late afternoon hours, insolation can still penetrate into the indoor space causing glare near windows.

2.4 Building orientation

BO is the building layout on a horizon plane or the sun's path pointing at an *AZM* angles between 0° and 360°. Typically, N is 0° or 360°, E is 90°, S is 180° and W corresponds to the 270°. The target of a proper BO is to avoid insolation impacts during summer and capture daylighting during winter. This approach is more evident in rectangular buildings [59]. Thus, well-oriented elongated shapes have been used widely in distinct climatic conditions [60]. Their larger façades oriented towards the underheated period results in daylighting enhancement during winter, while the shorter façades towards the overheated period controls excessive insolation during summer [61]. The smaller the surface area exposed to solar radiation, the more energy reduction for cooling can be achieved. Notably, the exposure of each façade to the sun in each hemisphere is different. Generally, façades facing to the S in the Northern Hemisphere and those facing N on the Southern Hemisphere are those struck by the higher sun's altitude during summer and the lower sun's altitude during winter [61][62]. Façades facing to the N-S receive twice the sunlight during winter, whilst those facing to the E-W get at least four times the value of insolation during summer [63][64]. A rectangular building in a summer sun's path in the Northern and Southern Hemispheres is illustrated in **Fig. 8** [65].

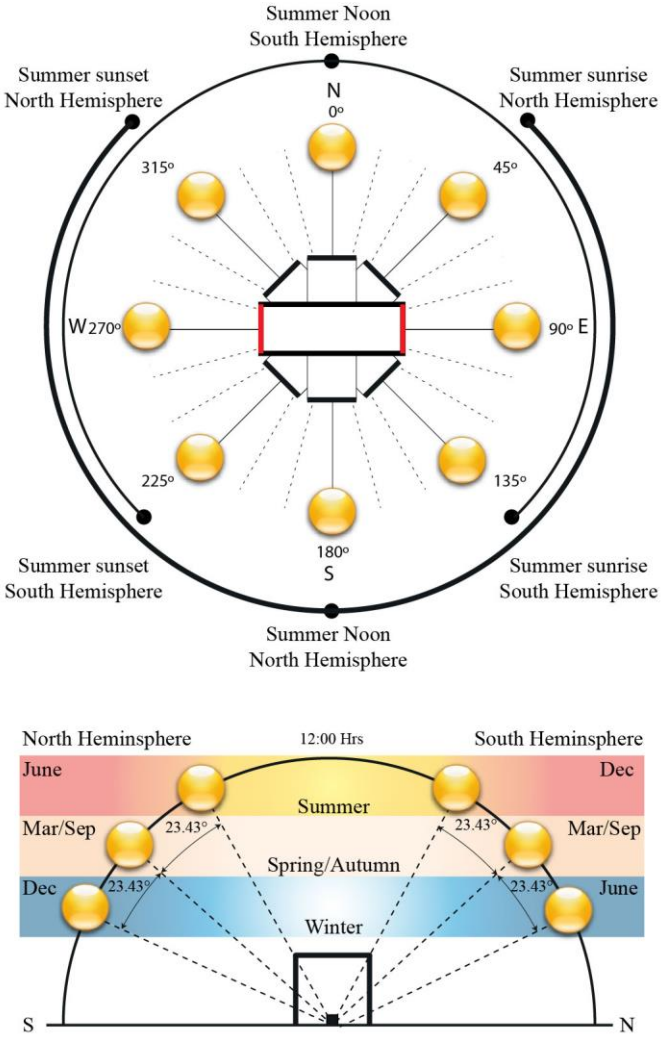

Fig. 8 Schematic plan and section in 2D view of a rectangular building in a summer sun's path in the Northern and Southern Hemispheres [65].

A sun emulator tool known as the Heliodon was traditionally used to find the proper BO [66]. Nowadays, sun-path projection software is used to examine the season's variations and sun altitude [67]. The proper BO accounting for the total energy gained by solar radiation on various shapes can be calculated using Eq. (9) [2]:

$$E = A \times \int_{\omega_1}^{\omega_2} (0.834 \times M) \times \left(\frac{\cos i}{\cos \theta_z}\right) d\omega \qquad (9)$$

Where, A is the surface area, M is the monthly mean daily global radiation on a horizontal surface, i is the incidence angle, ω_1 and ω_2 are the hour angles at sunrise

and sunset, θ_z is the zenith angle which is the imaginary line between the observer and the sun [2].

The effectiveness of a proper BO to decrease insolation and reduce energy demands were explored in Kuwait [68], Nigeria [69], Ghana [70] and Hong Kong [71]. A residential house in a suburban area of Kuwait City was able to reduce its energy loads by applying passive strategies such as a proper BO, shape, glazing, buffer zones and SDs. Al-Anzi and Khattab [68] reported that in a BWh climate during the peak months, the existing house with a large glazing area orientated to the SE and SW achieves higher demands on total cooling loads compared to a new building. To minimise the solar heat gains, a new hexagonal case was designed with large façades orientated to the N-S direction (see **Fig. 8**). In addition, it had overhangs on the N glazing, blinds on the S glazing and buffer zones on the E and W façades. This case was able to reduce the total cooling load by 0.05 kWh/m^2 (43%) during August. The usage of solar protection on the S, E and W façades clearly minimizes the impact of insolation on opaque and glazing elements. Similarly, in an institutional building located in the urban area of Ibadan, Nigeria, Odunfa et al. [69] investigated the effect of proper BO and its incidence on energy demands. They found that in an Aw climate, the solar heat gains were increased mainly through the fenestration areas on the E and W façades. After the larger façades of the rectangular building were orientated to the N and S, the total loads were reduced by 7.96 kWh/y (4.87%). Apart from reducing the energy demands, the proper BO also improved the daylighting and ventilation, which enhanced the indoor thermal comfort. The effects of proper the BO and glazing on cooling loads were also examined in an urban district of Kumasi, Ghana. In an Aw climate, the findings indicated that in a sun's path, by rotating the N façade of a rectangular building in steps of 90° from 0° to 360°, the cooling loads increased or

decreased depending on its orientation. A rectangular building located in the district of Bohyen, Ghana showed that when its larger façades were orientated to an *AZM* angle of 270° the solar insolation and energy capacity was increased. On the contrary, when façades pointed to an *AZM* angle of 0°, 360° or 180°, the cooling loads were reduced by 1.57 kWh/m^2/y (16.02%) [70]. Evidently, the building rotation at this location successfully lowers the building energy loads. Another study explored the influence of a proper BO and the shape of a high-rise residential building located in an agglomerated urban configuration like Hong Kong, China. The researchers identified that in a Cwa climate, the top floors of the rectangular building with its larger façades orientated to the E-W had higher cooling loads, mainly because they received a large amount of insolation and had less adjacent shading from surrounding buildings. Conversely, when the larger façades were orientated to the N-S, the building's total annual sensible cooling load was reduced by 11.18 kWh/m^2/y (19.76%) [71]. Similar cases have shown that high-rise buildings are prompt to receive higher insolation mainly on roofs, followed by the E and W walls and finally the N and S walls. These last two receive solar radiation depending on the location and seasonal variation. Therefore, the smaller the surface area of the opaque and glazing elements oriented to the E and W façades, the lower the energy demands.

3. Results and discussion

This section presents the results of the reviewed passive cases, which were analysed, discussed and evaluated. The performance of the FSS, SDs, WWR and BO vary from one case to another because they might be sensitive to factors such as geographical location, seasonal variations, local climate and envelope design [72][73]. To obtain the percentage range of the PES achieved by the passive cases, the EDR and PES are

summarised in **Table 2.**

Table 2 Summary of EDR and PES achieved by the passive cases.

Class	Ref.	Country and city	Cli-mate	Base cases	Area	Method	Period	Passive strategy		Passive cases	
								Design	Type	EDR	PES
Façade self-shading (FSS)	[30]	Israel, Jerusalem	Csa	Mid-rise office prismatic building total 7-storey	49.6 m^2/ floor	Modelling SustArc, Simulation Energy	Annual	Simple	Mixed	0.64 kWh/m^2/y	43%
	[31]	Greece, Athens	Csa	Low-rise office semi-prismatic building total 2-storey	N.A	Simulation Energy, WinAir	Annual	Simple	Single	40.8 kWh/y	4.64%
	[32]	China, Hong Kong	Cwa	Low-rise office prismatic building total 1-storey	2304 m^2/ floor	Simulation EnergyPlus	Annual	Simple	Single	7.51 kWh/m^2/y	10.95%
Shading devices (SDs)	[47]	Taiwan, Taipei	Cfa	High-rise office rectangular building total 18-storey	1325 m^2/ floor	Modelling Revit, Simulation Ecotect	Annual	Simple	Single	16.73 kWh/m^2/y	8.92%
	[48]	South Korea, Seoul	Dwa	Mid-rise residential rectangular building total 8 units per floor	150 m^2/ S-unit	Simulation Ecotect, DaySim, DOE-2.1E	May-Sept	Simple	Single	14.81 kWh/m^2	19.70%
	[49]	Singapore, Singapore	Af	High-rise residential rectangular building total 20-storey	628 m^2/ floor	Simulation eQUEST	Annual	Simple	Single	N.A	7.20%
	[50]	South Korea, Seoul	Dwa	High-rise residential rectangular total 20-storey	145 m^2/ unit	Simulation IES_VE, Radiance, CFD	Annual	Complex	Single	22.68 kWh/m^2/y	66%
Window wall ratio (WWR)	[55]	Turkey, Antalya	Csa	Low-rise residential square building total 3-storey	200 m^2/ 2-unit	Simulation SUNCODE-PC	Annual	Simple	Single	36.11 kWh/m^2/y	54.17%
	[56]	China, Guiyang	Cwa	Low-rise hotel square building total 3-storey	N.A	Simulation DeST	Annual	Simple	Single	114,429 kWh/y	53.98%
	[57]	Chile, Santiago	BSk	Mid-rise office square building total 10-storey	256 m^2/ floor	Modelling Ecotect, Simulation, DaySim, Radiance	Annual	Simple	Mixed	82.4 kWh/m^2/y	76.57%
	[58]	Norway, Oslo	Dfc	Low-rise office square single-person cubicle total 1-storey	10.5 m^2/ S-unit	COMFEN, Simulation EnergyPlus	Annual	Simple	Mixed	52 kWh/m^2/y	27.95%
Building orientation (BO)	[68]	Kuwait City, Kuwait	BWh	Low-rise residential hexagonal house total 2-storey	707 m^2/ floor	Simulation VisualDOE	Aug.	Complex	Mixed	0.05 kWh/m^2	43%
	[69]	Nigeria, Ibadan	Aw	Low-rise institutional square building total 2-storey	N.A	CLTD/CLF method	Annual	Simple	Single	7.96 kWh/y	4.87%
	[70]	Ghana, Bohyen	Aw	Low-rise residential rectangular building total 1-storey	137 m^2/ floor	Simulation EDSL 2008	Annual	Simple	Single	1.57 kWh/m^2/y	16.02%
	[71]	China, Hong Kong	Cwa	High-rise residential rectangular building total 40-storey	30,400 m^2/ block	Simulation EnergyPlus Shadow Algorithm	Annual	Simple	Single	11.18 kWh/m^2/y	19.76%

The results show that by decreasing the insolation on the building envelope, all passive cases were able to achieve EDR, which resulted in PES for HVAC systems. The percentage range of the PES achieved within the 15 passive cases varied from 4.64% to 76.57%.

In order to reveal the suitability of the selected passive strategies, the PES achieved by each passive case was classified by location and climate. Globally, from the 15 passive cases, 14 cases were located in the Northern and one in the Southern Hemisphere. The other 14 cases were mainly located within the tropical (TROP) and subtropical zones (SUBT), rather than the temperate zone (TEMP). The FSS class presented three cases all in the SUBT: one in a Cwa climate and two in a Csa climate. The SDs class showed four cases: one in the TROP, one in the SUBT and two in the TEMP. The WWR class exposed four cases: three in the SUBT and one in the TEMP. The BO class included four cases: two in the TROP and two in the SUBT. Finally, the case in the Southern Hemisphere was located within the SUBT zone [74][75]. **Fig. 9** shows the PES achieved by each passive case classified by location and climate [74][75]**.**

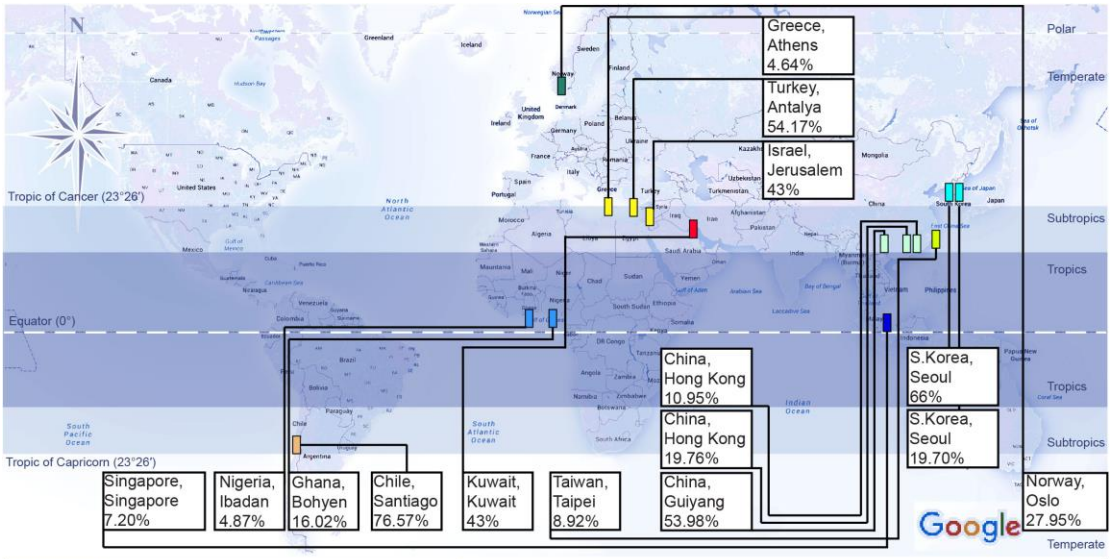

Hemisphere	NORTH		SOUTH	NORTH					
Zone	TROPICAL		SUBTROPICAL					TEMPERATE	
Climate	Af	Aw	BSk	BWh	Cfa	Cwa	Csa	Dwa	Dfc
	tropical rainforest no summer no winter	tropical savanna summer wet season winter dry season	semiarid steppe cold	arid desert hot	temperate no dry season hot summer	temperate dry winter hot summer	mediterranean dry summer hot summer	continental dry winter hot summer	continental subarctic no dry season cold summer
FSS	--	--	--	--	--	10.95%	43% 4.64%	--	--
SDs	7.20%	--	--	--	8.92%	--	--	19.70% 66%	--
WWR	--	--	76.57%	--	--	53.98%	54.17%	--	27.95%
BO	--	4.87% 16.02%	--	43%	--	19.76%	--	--	--

Fig. 9 PES achieved by each passive case classified by location and climate [74][75].

The passive strategies selected for each of the cases were considered suitable when their PES surpassed 40%. Five of such cases were found in the SUBT, one in the TEMP, but none were found in the TROP. It was observed that some cases located in the same city, with the same climate and with a similar strategy, obtained completely different results. Therefore, the PES might not only depend on climatic conditions but also on their geometry and application.

To identify the more effective combinations of passive strategies, the PES achieved by each passive case were analysed by performance. Each passive strategy has two components: its design and its type. The strategy design refers to its geometry, which is either simple or complex. The strategy type implies its application, either alone as a single strategy or mixed with other passive strategies. Of the 15 cases, 13 had simple

designs and only two had complex designs. In terms of strategy type, 11 cases were used as a single strategy while four cases were mixed with other passive strategies. The PES achieved by each passive case analysed by performance is depicted in **Fig 10.**

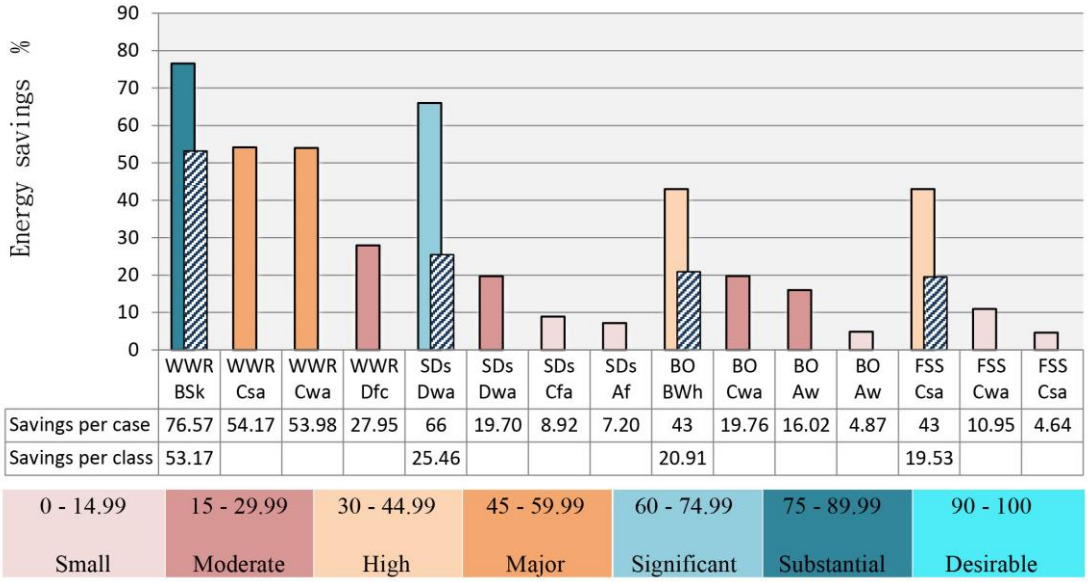

Fig. 10 PES achieved by each passive case analysed by performance.

The results of the analysis showed that within the WWR class, the combination of a simple design mixed with other passive strategies was effective when applied in a BSk climate within the SUBT. This combination was able to achieve substantial PES of up to 76.57%. Nevertheless, another simple design also mixed with other passive strategies was only able to obtain moderate PES of 27.95% within the TEMP. Additionally, other simple designs used as single strategies attained major PES of 53.98% and 54.17% within the SUBT. Furthermore, within the SDs class, a complex design used as a single strategy was effective when applied in a Dwa climate within the TEMP and accomplished significant PES of up to 66%. By contrast, the simple designs used as single strategies were only able to obtain small PES of 7.20% and 8.92% within the TROP and SUBT, as well as moderate PES of 19.70% within the TEMP. Continuously, within the BO class, the combination of a complex design mixed with other passive strategies was effective when applied in a BWh climate

within the SUBT and reached high PES of up to 43%. Additionally, the well-oriented simple designs used as single strategies obtained small PES of 4.87% within the TROP and moderate PES of 16.02% and 19.76% within the TROP and SUBT, respectively. Finally, within the FSS class, the combination of a simple design mixed with other passive strategies was found to be effective when applied in a Csa climate within the SUBT and gained high PES of up to 43%. By contrast, the other simple designs used as single strategies attained small PES of 4.64% and 10.95% also in the SUBT. As was observed, the more effective combinations of passive strategies were simple designs of WWR and FSS mixed with other passive strategies, which achieved substantial PES of 76.57% and high PES of 43%. A simple design of the WWR used as a single strategy gained major PES of 54.17%. A complex design of SDs used as a single strategy obtained significant PES of 66%. A complex design within the BO as a mixed strategy reached high PES of up to 43%. Therefore, the PES might not only depend on a combination of strategies but also on the accurate design of their parameters.

In order to establish which design parameter strongly influences the PES, each strategy type was classified by PES and categorised by its parameters. The design parameter of the WWR is the aperture percentage or glazing ratio in relation to the wall. Within the SDs class, the dominant parameter is the *VSA* of the devices and slats. Other parameters related to the design of SDs are their length, height, depth followed by their alignment, position and placement (internal or external). Within the BO class, the parameters that can alter the PES are the wall's length and height in relation to their *OSN* or the *AZM* angles to where they are facing. Within the FSS class is the wall's tilt in $\hat{Z}$, taken from the zenith to the sun's altitude, and the wall's tilt in $\tilde{V}$,

taken from the horizontal floor to the wall (see **Fig.4 (l)**). **Table 3** shows each strategy type classified by the PES and categorised by its parameters**.**

Table 3 Strategy types classified by the PES and categorised by its parameters.

Ref	Class	Zone	Cli-mate	Strategy type by PES		Strategy type by parameters							
						wall geometry		wall size		shading design			glazing ratio
				single %	mixed %	shape	$\hat{Z}$, $\tilde{V}$ angles	length large	length short	position alignment	*VSA* angles	place-ment	aperture %
[55]	WWR	SUBT	Csa	54.17	-	square	all 90°	-	-	-	-		25
[56]	WWR	SUBT	Cwa	53.98	-	square	all 90°	-	-	-	-		25
[57]	WWR	SUBT	BSk	-	76.57	square	all 90°	-	-	horizontal internal blinds	- -	N E,W	20
[58]	WWR	TEMP	Dfc	-	27.95	square	all 90°	-	-	-	-		41
[47]	SDs	SUBT	Cfa	8.92	-	rectangular	all 90°	-	-	horizontal	-	N,S, E,W	-
[48]	SDs	TEMP	Dwa	19.70	-	rectangular	all 90°	-	-	horizontal	-	S	-
[49]	SDs	TROP	Af	7.20	-	rectangular	all 90°	-	-	overhang tilt	30°	W	-
[50]	SDs	TEMP	Dwa	66.00	-	rectangular	all 90°	-	-	overhang tilt slats tilt	- 60°	- S	-
[68]	BO	SUBT	BWh	-	43.00	hexagonal	all 90°	N-S	E-W	horizontal internal blinds open buffer zones	- -	N S E, W	-
[69]	BO	TROP	Aw	4.87	-	rectangular	all 90°	N-S	E-W	-	-		-
[70]	BO	TROP	Aw	16.02	-	rectangular	all 90°	N-S	E-W	-	-		-
[71]	BO	SUBT	Cwa	19.76	-	rectangular	all 90°	N-S	E-W	-	-		-
[30]	FSS	SUBT	Csa	-	43.00	prismatic	S-31° W-34° E-34°	-	-	internal blinds	-	W	-
[31]	FSS	SUBT	Csa	4.64	-	semi-prismatic	S-143° W-7° E-4°	-	-	-	-	-	-
[32]	FSS	SUBT	Cwa	10.95	-	prismatic	all 40°	-	-	-	-	-	-

The results of this analysis showed that the design parameters that strongly influence the PES varied from one case to another. Within the WWR class, the case located in a BSk climate in the SUBT achieved substantial PES of 76.57%, due to its low glazing ratio of 20%, an additional horizontal overhang on the N and internal blinds on the E and W sides. A case within the SDs class, located in a Dwa climate in the TEMP was able to accomplish significant PES of 66%, because the S-side of the building included tilted overhangs and slats with *VSA* equal to 60°. A case within the BO class, located in a BWh climate in the SUBT obtained high PES of 43%, due to its larger

façades orientated to the N-S and its shorter façades to the E-W, which also had a horizontal overhang on the N side, internal blinds on the S side and buffer zones on the E-W sides. A case within the FSS class, located in a Csa climate in the SUBT achieved high PES of 43%, because the wall on the W side of the building was designed with a $\hat{Z}$ of 34°, but with additional internal blinds. Except for one case within the SDs, which was designed with optimal parameters, the other effective cases improved their PES by protecting the S, E and W sides, but with internal blinds. Evidently, internal blinds were effective at blocking the insolation, but unfortunately they also reduced daylighting, visibility and still let shortwave radiation pass through the glass. Therefore, as an alternative to internal blinds, other strategy types were evaluated to recommend more effective and balanced solutions.

To recommend designs and parameters for developing more effective and balanced solutions, all strategy types were evaluated in terms of insolation, daylighting, visibility and PES. Within the WWR class, a simple design with a low glazing portion was able to decrease the insolation entering the interior space during noon time and partially during the early morning and late afternoon. However, low glazing ratios can also reduce the indoor daylighting and limit the visibility to the outside environment. Low WWRs accomplished PES up to 54.17% in the SUBT. The studies for sizing the WWRs for each orientation are limited, but low or full glazing ratios need to be well insulated or shaded or made of efficient materials. Within the SDs class, simple designs such as horizontal projections are restricted to diminish insolation over glazing elements but only during noon time. On the contrary, complex designs with proper *VSA* are able to block insolation all day. The amount of daylighting passing through a complex design with slats depends on their design parameters. These parameters also control the degree of visibility to the outdoors. Simple designs of SDs

accomplished PES up to 19.70%, whilst complex designs raised the PES up to 66%, both in the TEMP. Further studies to determine other complex designs of SDs with accurate parameters for each façade in different locations and climates are needed. Within the FSS class, the simple designs with inclined walls can diminish the insolation over opaque and glazing elements. The distribution of daylighting using simple designs during noon time can be even, but they can also cause glare discomfort during early morning or late afternoon. Nevertheless, all simple designs offer good visibility compared to complex designs, which need to be highly designed to keep acceptable levels of visibility. Simple designs of FSS achieved PES of up to 10.95% in year-round hot climates in the SUBT. Clearly, there is still a need to evaluate complex designs of FSS and their design parameters in different locations and climates. Within the BO class, simple or complex shapes with a proper wall size facing each orientation can decrease insolation and slow down heat gains. The levels of daylighting in a well-oriented building can be maximised during winter months, but during summer months, certain façades might need solar protection, which must be adjusted to the geographical location. The visibility in a well-oriented building might further depend on additional strategies and their design parameters. Simple designs with proper BO were able to obtain PES of up to 19.76%, which could be further increased by adding other strategies. Consequently, more studies are needed to investigate complex shapes and their proper BO in different locations and climates.

Overall, this research recommends the use of complex designs of FSS and SDs with the accurate design of their parameters $\hat{Z}$, $\tilde{V}$ and *VSA* as the most effective solutions for decreasing insolation, while balancing daylighting, visibility and PES. A rectangular building oriented optimally can control the insolation received by the building surfaces during summer and winter seasons. Complex designs are more

suitable for building façades that are heavily struck by insolation during the summer months. In addition, the design of their parameters should be adjusted on each façade according to the geographical location. Complex designs of FSS and SDs are permanent solutions, and their strategic placement must be planned from the beginning of the project to increase their efficiency. Additionally, in hot climates such complex designs can be useful for the integration of RSCT, which can maximise building cooling performance.

4. Filling the gap: Optimal building orientation for the strategic placement of complex and simple designs of façade self-shading and shading devices

As has been shown in the present review, every energy-efficient building begins with a proper building shape and optimal building orientation (OBO). These two basic strategies enhance energy savings and environmental aspects from early stages of planning and design [76]. A rectangular building oriented optimally has a better control over the amount of insolation reaching its façades [77]. The knowledge of which façades are optimal for solar protection (OBOSP) during summer and which ones are optimal for solar collection (OBOSC) during winter are crucial indicators for planning the strategic placement of complex and simple designs. There is still a lack of comprehensive data on this matter [78][79][80]. In order to determine optimal façades for the strategic placement of complex and simple designs of FSS and SDs, a worldwide guide of azimuth angles are calculated and classified by orientation.

4.1 Simulation method

Nowadays, computer software can speed up the procedure to find the OBO for planning and design decisions [81]. Ecotect® is analysis software for designing energy efficient buildings, which can accurately load weather data, find geographical

location, calculate *AZM* angles, determine the sun's altitude, compute solar and shading gains on the building fabric and perform energy simulations [82]. This study used Weather Tool from Ecotect® to obtain the accurate weather data for each location and to calculate the optimal *AZM* angles for OBOSP and OBOSC worldwide. By using the option to convert weather data from Ecotect®, the epw (energy plus weather) file [83] was imported, converted and exported as a wea (weather data) file. Ecotect® displays the wea files providing precise information about solar radiation and weather conditions on an hourly, weekly and yearly basis [84][85]. Hourly data for the hottest and coldest days in each location was obtained and input into a stereographic diagram. For the calculation of the OBO, Weather Tool automatically determines in a year the three peak months during summer and winter. The values chosen for the overheated and underheated periods are the Julian dates in the year (1 to 365). The constraints for the calculation are that no month can belong to both groups and each period must be contiguous (see **Fig.11**). A stereographic diagram used to calculate the OBO assumes a fictitious rectangular surface, which would rotate 360° [86]. The calculation is derived from the amount of insolation that reaches the vertical surfaces on $1m^2$ for each 5° rotation on a 360° sun's path [87]. Finally, based on the total insolation received on the building surfaces during the entire year, the three hottest and coldest months, the stereographic diagram indicates the optimal *AZM* angles to where façades should be oriented to improve shading and daylighting at the same time (see **Fig.12**) [82].

4.2 Case study: Hong Kong

Hong Kong is located in Asia continent, lies between latitude 23°10' N and longitude 113°20' E. Hong Kong's climate is classified as Cwa [74]. Annual insolation based on peak summer and winter months in Hong Kong are shown in **Fig. 11**[82]**.**

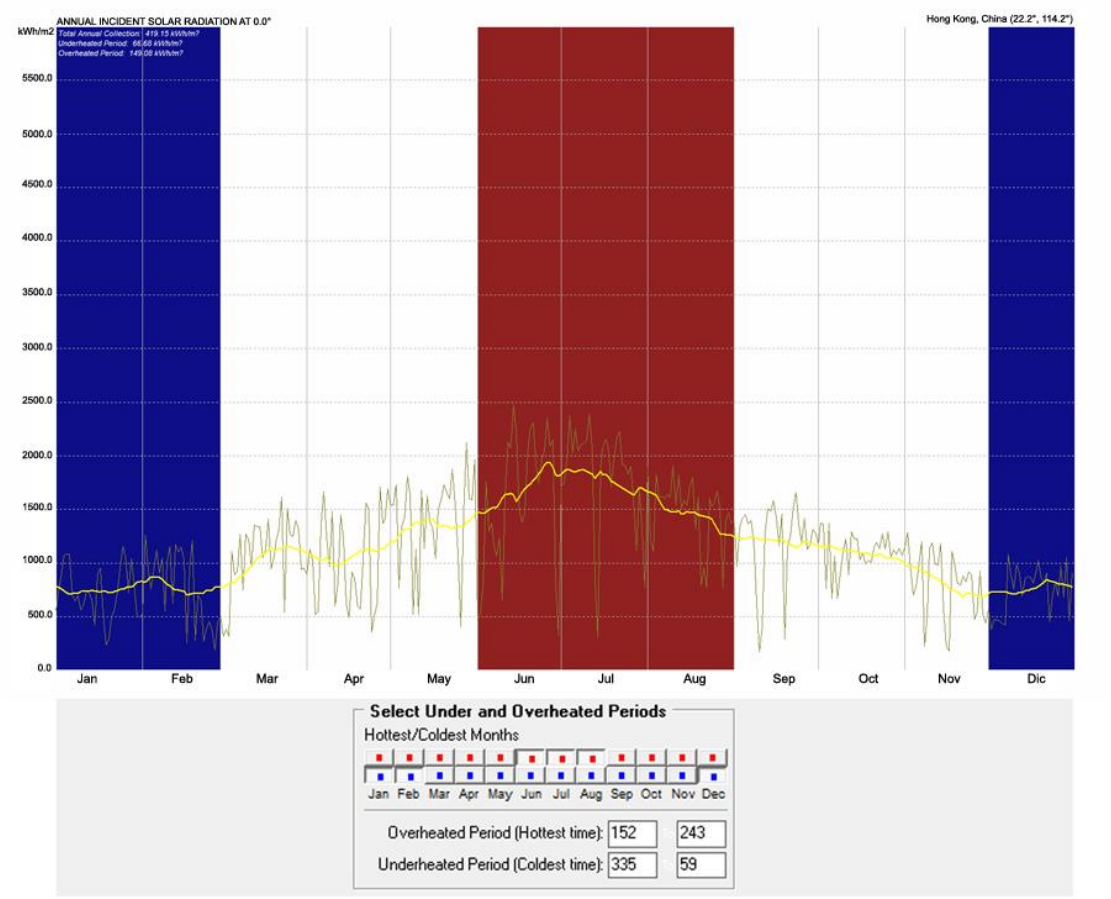

Fig. 11 Elevation in 2D view of the annual insolation based on peak summer and winter months in Hong Kong [82].

As can be seen, the overheated period is during June to August (152 to 243) and the underheated period starts in December until end of February (335 to 59).

Fig. 12 shows the stereographic diagram with the *AZM* angles found for OBOSP and OBOSC in Hong Kong [82].

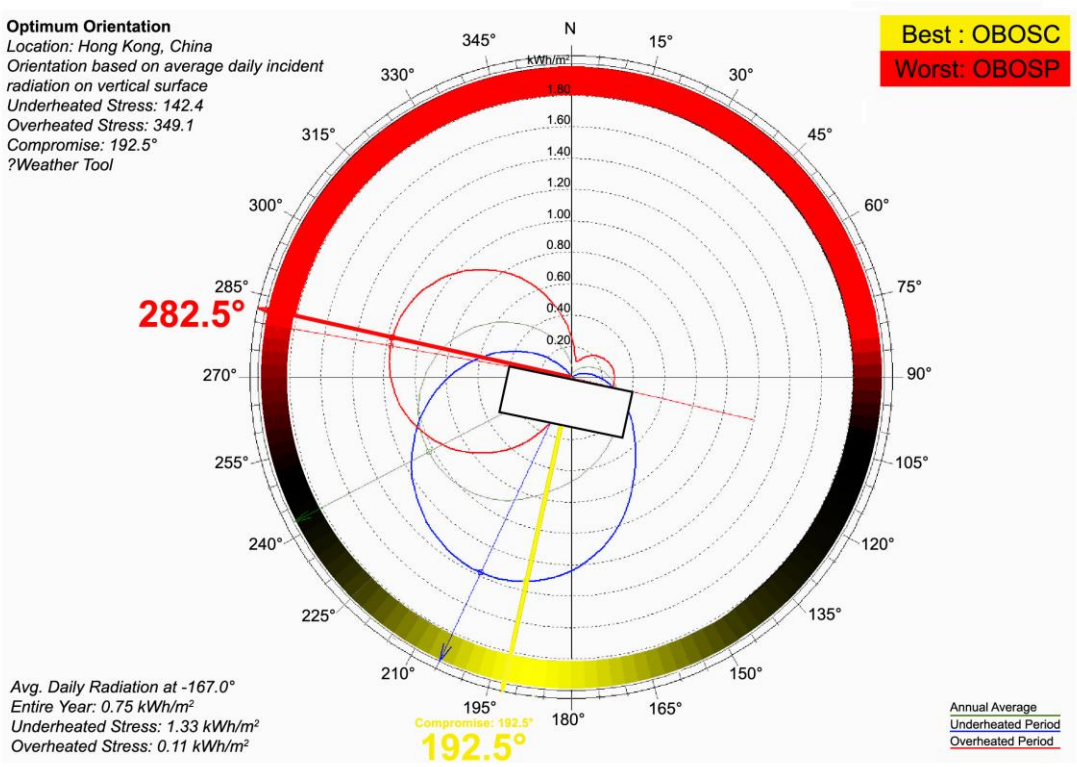

Fig. 12 Top 2D view of the stereographic diagram with the *AZM* angles found for OBOSP and OBOSC in Hong Kong [82].

The *AZM* angles found for OBOSP and OBOSC in a rectangular building located in Hong Kong showed that the shorter façade pointing to an *AZM* angle of 282.5° is optimal for the strategic placement of complex designs of FSS and SDs, which will provide maximum shading during summer. However, the larger façade pointing to an *AZM* angle of 192.5° is optimal for applying simple designs that will provide shading during summer but maximum daylighting during winter.

4.3 Worldwide guide of azimuth angles

This section provides the *AZM* angles, to determine the optimal façades for the strategic placement of complex and simple designs in other cities. A total of 82 locations [83] and 28 climate types [74] were selected. No cities in Dsa or Dsd climates were found, and no weather data was available for 23 cities. Consequently, the calculation of *AZM* angles to find the OBOSP and OBOSC was carried out in 59

locations. The worldwide guide of *AZM* angles found for OBOSP and OBOSC is shown in **Table 4** [74][83].

Table 4 Worldwide guide of *AZM* angles found for OBOSP and OBOSC [74][83].

Climate	Type	Hemi-sphere	Location		Country	City	*AZM* angles			
			latitude	longitude			OBOSP overheated short façade		OBOSC underheated large façade	
Af	tropical rainforest no summer no winter	NH	3.10	101.70	Malaysia	Kuala Lumpur	127.5°	SE	37.5°	NE
		NH	1.40	104.0	Singapore	Singapore	75.0°	NE	165.0°	SE
		NH	26.70	-80.10	United States	W. Palm Beach	87.5°	E	177.5°	S
		SH	-7.20	112.70	Indonesia	Surabaya	-	-	-	-
Am	tropical monsoon large rainy season short dry season	NH	25.70	-80.20	United States	Miami	260.0°	W	170.0°	S
		SH	-6.10	106.70	Indonesia	Jakarta	-	-	-	-
		NH	16.00	108.20	Vietnam	Da Nang	-	-	-	-
		SH	-5.10	119.40	Indonesia	Makassar	-	-	-	-
Aw	tropical savanna summer wet season winter dry season	SH	-15.90	-47.90	Brazil	Brasilia	57.5°	NE	327.5°	NW
		NH	19.10	72.80	India	Mumbai	107.5°	SE	17.5°	NE
		SH	-22.90	-43.20	Brazil	Rio de Janeiro	-	-	-	-
		NH	110.70	106.70	Vietnam	Ho Chi Minh	-	-	-	-
BWh	arid desert hot	NH	30.10	31.40	Egypt	Cairo	95.0°	E	185.0°	S
		NH	124.60	46.70	Saudi Arabia	Riyadh	82.5°	E	172.5°	S
		SH	-12.00	-77.10	Peru	Lima	70.0°	NE	340.0°	NW
		NH	29.2	48	Kuwait	Kuwait	90.0°	E	180.0°	S
BWk	arid desert cold	NH	35.30	-113.90	United States	Kingman	90.0°	E	180.0°	S
		SH	-23.40	-70.40	Chile	Antofagasta	95.0°	E	5.0°	N
		SH	-26.60	15.10	Namibia	Lüderitz	-	-	-	-
		SH	-32.88	-68.81	Argentina	Mendoza	-	-	-	-
BSh	semi-arid steppe hot	NH	28.50	77.20	India	New Delhi	100.0°	E	190.0°	S
		SH	-23.30	43.60	Madagascar	Tulear	-	-	-	-
BSk	semi-arid steppe cold	SH	-33.40	-70.80	Chile	Santiago	85.0°	E	355.0°	N
		NH	50.70	-120.40	Canada	Kamloops	75.0°	NE	165.0°	SE
		NH	47.90	107.0	Mongolia	Ulaanbaatar	82.5°	E	172.5°	S
		NH	38.00	46.20	Iran	Tabriz	80.0°	E	170.0°	S
Csa	mediterranean dry summer hot summer	SH	-34.90	138.60	Australia	Adelaide	272.5°	W	2.5°	N
		NH	43.70	7.20	France	Nice	80.0°	E	170.0°	S
		NH	37.90	23.70	Greece	Athens	72.5°	NE	162.5°	SE
		NH	41.80	12.60	Italy	Rome	82.5°	E	172.5°	S
Csb	mediterranean dry summer warm summer	NH	49.20	-123.10	Canada	Vancouver	77.5°	E	167.5°	S
		NH	37.70	-122.40	United States	San Francisco	280.0°	W	190.0°	S
		NH	47.60	-122.30	United States	Seattle	275.0°	W	185.0°	S
		NH	44.90	-123.00	United States	Salem	-	-	-	-
Csc	maritime subalpine dry summer cold summer	SH	-38.85	-71.69	Chile	Melipeuco	-	-	-	-
		SH	-45.90	-71.70	Chile	Balmaceda	-	-	-	-
Cwa	temperate dry winter hot summer	NH	23.10	113.20	China	Hong Kong	282.5°	W	192.5°	S
		NH	21.00	105.80	Vietnam	Hanoi	52.5°	NE	322.5°	NW
Cwb	maritime temperate dry winter warm summer	NH	19.40	-99.10	Mexico	Mexico City	105.0°	E	15.0°	N
		NH	4.70	-74.10	Colombia	Bogota	152.5°	SE	62.5°	NE
		SH	-26.10	28.00	South Africa	Johannesburg	95.0°	E	5.0°	N
		SH	-15.49	-70.12	Peru	Juliaca	-	-	-	-
Cwc	maritime temperate dry winter cold summer	SH	-16.50	-68.20	Bolivia	La Paz	102.5°	E	12.5°	N
		SH	-16.16	-69.08	Bolivia	Copacabana	-	-	-	-
Cfa	temperate no dry season hot summer	NH	31.20	121.40	China	Shanghai	80.0°	E	170.0°	S
		NH	25.10	121.50	Taiwan	Taipei	85.0°	E	175.0°	S
		NH	40.70	-73.90	United States	New York	272.5°	W	182.5°	S
		NH	45.40	12.30	Italy	Venice	67.5°	NE	157.5°	SE

Cfb	maritime no dry season warm summer	NH	46.20	6.10	Switzerland	Geneva	85.0°	E	175.0°	S
		NH	48.10	11.50	Germany	Munich	75.0°	NE	165.0°	SE
		NH	51.40	0.0	United Kingdom	London	82.5°	E	172.5°	S
		NH	-41.30	174.80	New Zealand	Wellington	95.0°	E	5.0°	N
Cfc	maritime subarctic no dry season cold summer	NH	57.80	-152.30	Alaska	Kodiak	82.5°	E	172.5°	S
		NH	64.10	21.90	Iceland	Reykjavik	82.5°	E	172.5°	S
Dsa	continental dry summer hot summer									
Dsb	continental dry summer warm summer	NH	47.60	-117.50	United States	Spokane	80.0°	E	170.0°	S
		NH	41.50	-71.30	United States	Newport	-	-	-	-
Dsc	continental subarctic dry summer cold summer	NH	61.10	-150.00	Alaska	Anchorage	282.5°	W	192.5°	S
		NH	60.60	-151.20	Alaska	Kenai	82.5°	E	172.5°	S
Dsd	continental subarctic dry summer very cold winter									
Dwa	continental dry winter hot summer	NH	41.50	123.80	China	Fushun	82.5°	E	172.5°	S
		NH	37.50	126.90	Korea	Seoul	67.5°	NE	157.5°	SE
		NH	39.80	116.50	China	Beijing	85.0°	E	175.0°	S
		NH	45.70	126.60	China	Harbin	-	-	-	-
Dwb	continental subarctic dry winter warm summer	NH	43.10	131.9	Russia	Vladivostok	-	-	-	-
		NH	51.10	-114.00	Canada	Calgary	82.5°	E	172.5°	S
Dwc	continental subarctic dry winter cold summer	NH	50.42	124.07	China	Jiagedaqi	-	-	-	-
Dwd	continental dry winter very cold winter	NH	63.46	142.78	Russia	Oymyakon	-	-	-	-
Dfa	continental no dry season hot summer	NH	41.80	-87.80	United States	Chicago	82.5°	E	172.5°	S
		NH	44.50	26.10	Romania	Bucharest	85.0°	E	175.0°	S
		NH	42.30	-83.00	Canada	Windsor	80.0°	E	170.0°	S
		SH	-33.05	-71.60	Chile	Valparaiso	-	-	-	
Dfb	continental no dry season warm summer	NH	52.20	21.00	Poland	Warsaw	75.0°	NE	165.0°	SE
		NH	55.70	37.60	Russia	Moscow	65.0°	NE	155.0°	SE
		NH	59.90	30.30	Russia	St. Petersburg	72.5°	NE	162.5°	SE
		NH	50.10	14.30	Czech Republic	Prague	82.5°	E	172.5°	S
Dfc	continental subarctic no dry season cold summer	NH	45.40	-73.70	Canada	Montreal	75.0°	NE	165.0°	SE
		NH	43.60	-79.60	Canada	Toronto	67.5°	NE	157.5°	SE
		NH	64.80	-147.90	Alaska	Fairbanks	85.0°	E	175.0°	S
		NH	64.50	40.60	Russia	Archangelsk	-	-	-	
Dfd	continental subarctic no dry season very cold winter	NH	62.10	129.80	Russia	Yakutsk	85.0°	E	175.0°	S
		NH	62.93	152.38	Russia	Seymchan	-	-	-	
ETf	polar tundra no dry season	NH	71.30	-156.70	Alaska	Barrow	80.0°	E	170.0°	S
		NH	60.14	-45.24	Greenland	Nanortalik	-		-	
Climate 28			Locations 82		Countries 40	Cities 82	Simulations 59			

To clearly visualise the relationship between the *AZM* angles and their orientation, the angles were divided into eight groups. A good orientation could have an angle variation of up to ±45° [2]. However, to be more accurate, this study uses a variation

of only ±15° from the four main orientations (N, S, E and W). The remaining *AZM* angles were grouped based on the highest and lowest values for the intermediate orientations [88]. **Table 5** shows the relationship between the *AZM* angle groups with their ideal orientations [2][88].

Table 5 Relationship between the *AZM* angle groups with their ideal orientations [2][88].

AZM angle group	346°~0°~15°	16°~75°	76°~90°~105°	106°~165°
Ideal orientation	N oriented	NE oriented	E oriented	SE oriented
AZM angle group	166°~180°~195°	196°~255°	256°~270°~285°	286°~345°
Ideal orientation	S oriented	SW oriented	W oriented	NW oriented

The *AZM* angles found for OBOSP show that of the 59 locations, 35 (58.62%) should apply complex designs to the E orientation, 14 (24.13%) to the NE orientation, seven (12.06%) to the W orientation and three (5.17%) to the SE orientation for solar protection. The *AZM* angles for OBOSP and ideal orientation worldwide are presented in **Fig. 13.**

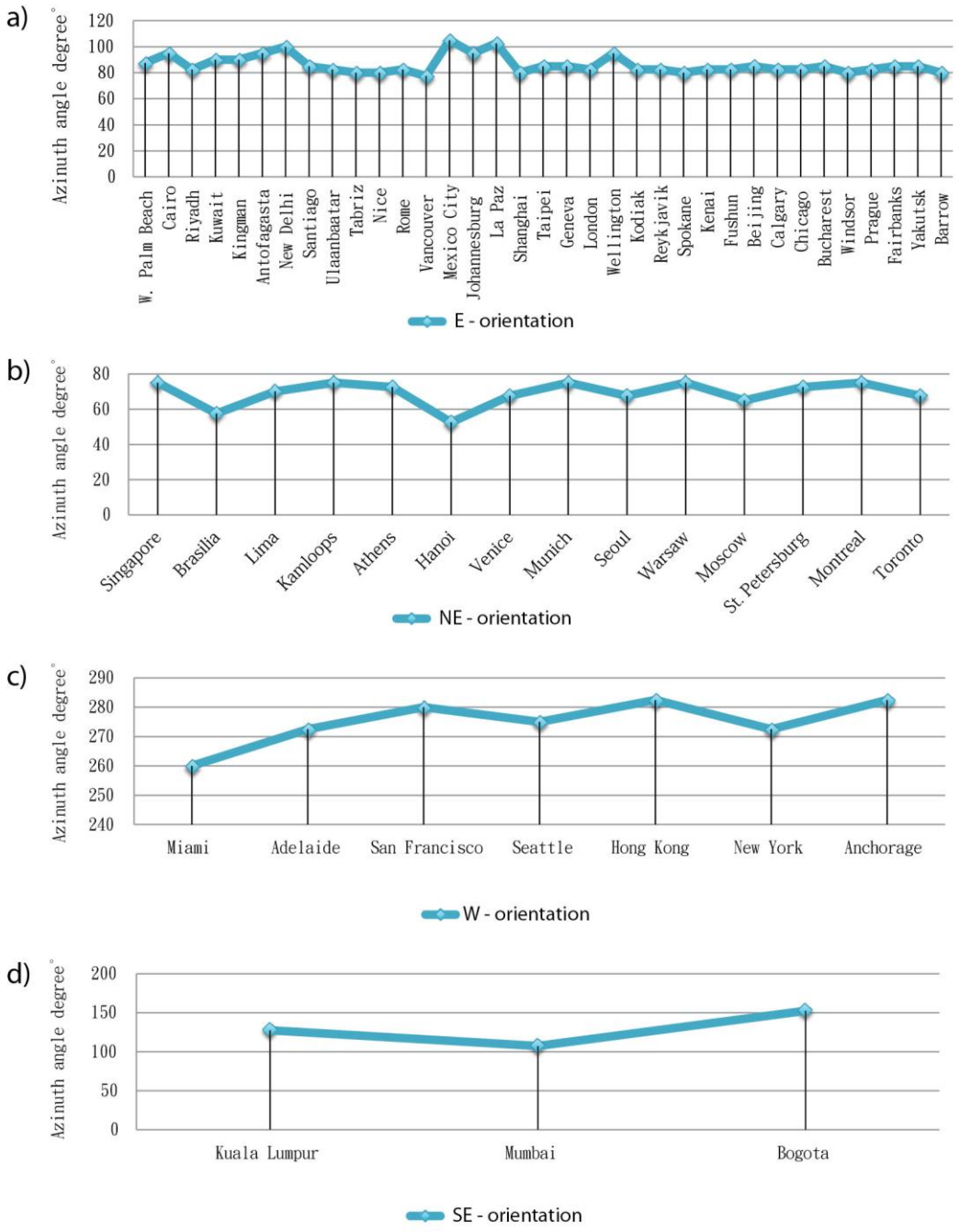

Fig. 13 *AZM* angles for OBOSP and ideal orientation worldwide: a) E orientation, b) NE orientation, c) W orientation and d) SE orientation.

Conversely, the *AZM* angles found for OBOSC show that of the 59 locations, 35 (58.62%) should apply simple designs to the S orientation, 11 (18.98%) to the SE orientation, seven (12.06%) to the N orientation, three (5.17%) on the NW orientation

and three (5.17%) to the NE orientation for solar protection and daylighting collection during summer and winter, respectively. **Fig. 14** presents the *AZM* angles for OBOSC and ideal orientations worldwide**.**

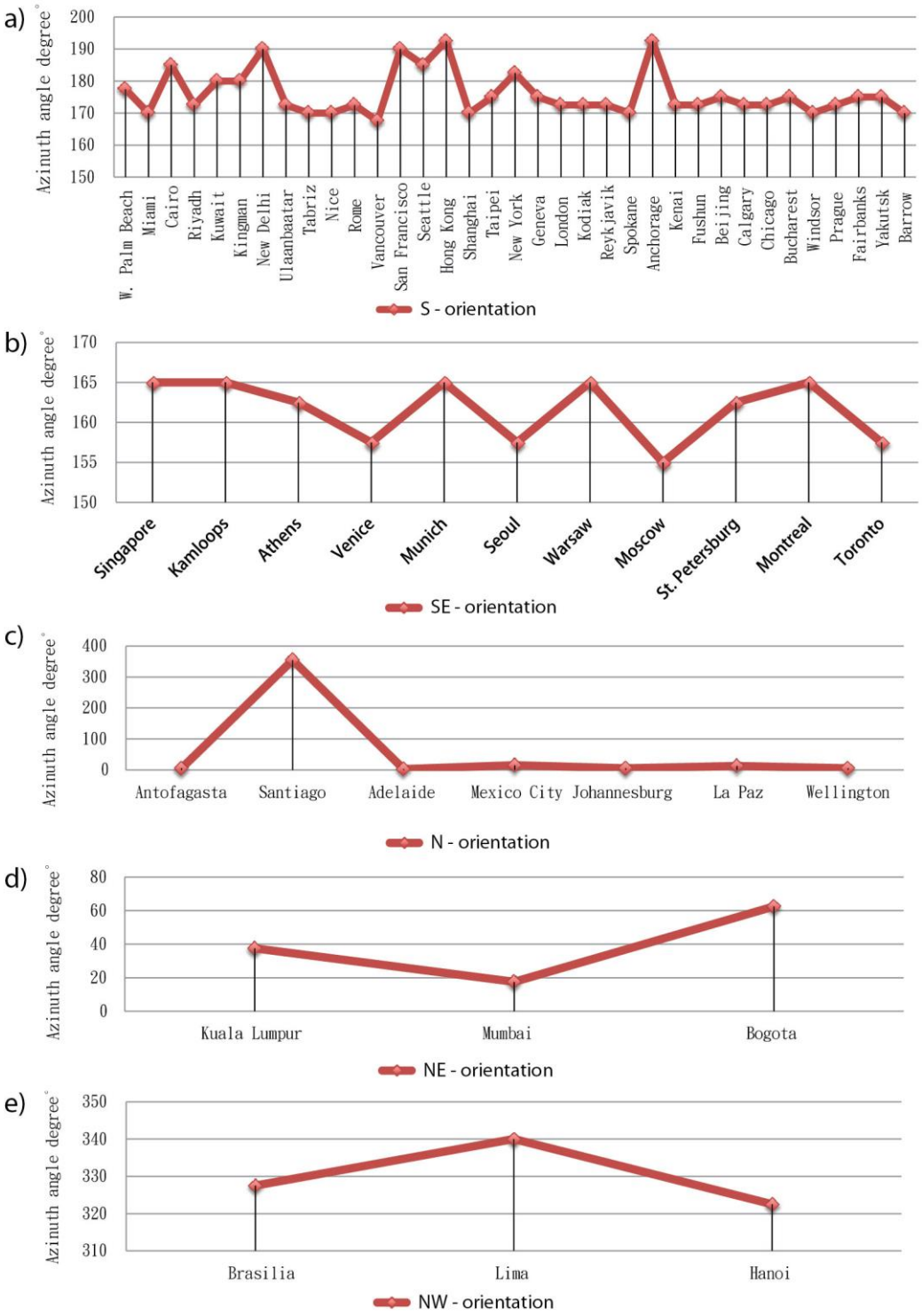

Fig. 14 *AZM* angles for OBOSC and ideal orientation worldwide: a) S orientation, b) SE orientation, c) N orientation, d) NE orientation and e) NW orientation.

The *AZM* angles of this guide are important indicators for maximising shading and daylighting and to help reduce energy demands. The *AZM* angles for OBOSP (**Table 4**) indicate the optimal façades (**Table 5**) for the strategic placement of complex designs of FSS and SDs. Following this, their design parameters, such as $\hat{Z}$, $\tilde{V}$ as well as *HSA* and *VSA*, can be accurately calculated (**Section 2**). Furthermore, complex designs of FSS (**Fig.4**) and SDs (**Fig.5**) can be used for the integration of RSCT [89][90][91], either transparent or semi-transparent [92] to maximise building cooling. The present research opens a large scale of possibilities for developing more effective and balanced designs for each façade in various locations and climate types, especially within the TROP and SUBT.

5. Conclusions

The aim of this research was to recommend the most effective passive solutions to decrease insolation and increase energy savings for cooling systems, while balancing daylighting and visibility. Their strategic placement and accurate design from the beginning of a project is essential to achieve desirable results. Therefore, this study additionally provides a worldwide guide of azimuth angles, to determine optimal façades for the strategic placement of effective and balanced solutions. The suggestions made in this study will be useful for developing more effective and balanced designs worldwide. The major findings are as follows:

1. Several cases within the FSS, SDs, WWR and BO classes were reviewed. All 15 cases with passive strategies were able to decrease insolation over the opaque and glazing elements and reduce energy demands. The EDR resulted in PES for HVAC systems, which varied from 4.64% to 76.57%.

2. The passive strategies selected for each of the cases were considered suitable when they surpassed PES of 40%. Five such cases were found in the SUBT, one in the TEMP, but none in the TROP.

3. The effective combinations of strategies like simple designs of WWR and FSS mixed with other passive strategies achieved substantial PES of 76.57% and high PES of 43%. A simple design of the WWR accomplished major PES of 54.17%. A complex design of SDs used as a single strategy obtained significant PES of 66%. A complex design of BO as a mixed strategy attained high PES of up to 43%.

4. The design parameters that strongly influenced the PES of the SDs were their proper application and design. The PES within the WWR, FSS and BO classes were influenced by using internal blinds on the S, E and W sides, which unluckily blocked the daylighting, visibility and still let shortwave radiation pass through the glass.

5. As an alternative to internal blinds, the most recommended solutions are complex designs of FSS and SDs. Their strategic placements and the accurate design of their parameters such as *HSA* and *VSA* as well as the $\hat{Z}$ and $\tilde{V}$ angles, maximise their performance.

6. The knowledge of which façades are optimal for solar protection during summer and which ones are optimal for solar collection during winter are crucial indicators for planning the strategic placement of complex and simple designs of FSS and SDs.

7. The *AZM* angles found for OBOSP show that of the 59 locations, 58.62% should apply complex designs to the E orientation, 24.13% to the NE orientation, 12.06% to the W orientation and 5.17% to the SE orientation for solar protection.

8. Similarly, the *AZM* angles found for OBOSC show that of the 59 locations, 58.62% should apply simple designs to the S orientation, 18.98% to the SE orientation, 12.06% to the N orientation, 5.17% to the NW orientation and 5.17% to the NE

orientation for solar protection and daylighting collection during summer and winter, respectively.

9. More research on complex designs combined with other strategies is needed to determine suitable solutions for each façade in other locations and climates.

10. Each zone on Earth receives different amounts of sunlight, which is a key factor in determining the cooling or heating requirements. Complex designs optimally oriented can be used for the integration of RSCT to maximise building cooling in the TROP and SUBT.

The findings of this research will significantly increase awareness among municipalities, developers, architects, engineers, builders, designers and all experts within the building design industry, who are willing to make the best energy saving decisions from the early planning and design stages. The findings presented might have a global impact by decreasing the energy consumption of cooling equipment, which will gradually lead to highly energy-efficient buildings and sustainable city development.

Acknowledgements

The author would like to thank the Department of Urban Development and Urban Planning Taipei City Government for their suggestions and cooperation.

References

[1] ⟨http://buildingsdatabook.eren.doe.gov/TableView.aspx?table=1.1.13⟩ U.S. Department of Energy (DOE). Building energy data book; 2012. [Visited 31.10.2016].

[2] Pacheco R, Ordóñez J, Martínez G. Energy efficient design of building: A review. Renewable Sustainable Energy Rev. 2012;16:3559-3573.

[3] European Comission - Fact Sheet (EUC). Towards a smart, efficient and sustainable heating and cooling sector 2016. Governemnt of Brussels; 2016.

[4] Santamouris M. Cooling the buildings – past, present and future. Energy Build. 2016;128:617-638.

[5] Farrou I, Kolokotroni M, Santamouris M. Building envelope design for climate change mitigation: a case study of hotels in Greece. Int. J. Sustainable Energy. 2016;35:944-967.

[6] Galiano A, Nocera F, Patania F, Moschella A, Detommaso M, Evola G. Synergic effects of thermal mass and natural ventilation on the thermal behaviour of traditional massive buildings. Int. J. Sustainable Energy. 2016;35:411-428.

[7] Sharifi E, Lehmann S. Comparative analysis of surface urban heat island effect in central Sydney. Int. J. Sustainable Dev. 2014;7:23-34.

[8] ⟨https://www.wbdg.org/resources/gbs.php⟩ Vierra S. Green building standards and certification systems. National Institute of Building Sciences (NIBS); 2014. [Visited 31.10.2016].

[9] Talen E, Allen E, Bosse A, Ahmann J, Koschinsky J, Wentz E, et al. LEED-ND as an urban metric. Landscape Urban Plann. 2013;119:20-34.

[10] Pérez-Lombard L, Ortiz J, Coronel JF, Maestre IR. A review of HVAC systems requirements in building energy regulations. Energy Build. 2011;43:255-268.

[11] Wang Q, Zhang M. Introduction of the standard for energy efficient building evaluation. Sustainable Cities Soc. 2015;14:1-4.

[12] ⟨http://www.enviroarch.com/tiers.html⟩ Goldman D. Progressive environmental design solutions. Environmental Architecture; 2016. [Visited 31.10.2016].

[13] Rodriguez-Ubinas E, Montero C, Porteros M, Vega S, Navarro I, Castillo-Cagigal M, et al. Passive design strategies and performance of Net Energy Plus Houses. Energy Build. 2014;83:10-22.

[14] ⟨http://energy.gov/energysaver/passive-solar-home-design⟩ U.S. Department of Energy (DOE). Passive solar home design. 2016. [Visited 31.10.2016].

[15] ⟨http://www.designingbuildings.co.uk/wiki/Passive_building_design⟩ Institutuion of Civil Engineers (ICE). Designing Buildings Wiki: Passive building design. 2016. [Visited 31.10.2016].

[16] Voss K, Herkel S, Pfafferott J, Löhnert G, Wagner A. Energy efficient office buildings with passive cooling – Results and experiences from a research and demonstration programme. Sol. Energy. 2007;81:424-434.

[17] Harvey D. Reducing energy use in the buildings sector: measures, costs, and examples. Energy Effic. 2009;2:139-163.

[18] Geetha NB, Velraj R. Passive cooling methods for energy efficient buildings with and without thermal energy storage – A review. Energy Education Science and Technology Part A: Energy Science and Research. 2012;29(2):913-946.

[19] Lotfabadi P. High-rise buildings and environmental factors. Renewable Sustainable Energy Rev. 2014;38:285-95.

[20] Gago EJ, Roldan J, Pacheco-Torres R, Ordóñez J. The city and urban heat islands: A review of strategies to mitigate adverse effects. Renewable Sustainable Energy Rev. 2013;25:749-758.

[21] Sadineni SB, Madala S, Boehm RF. Passive building energy savings: A review of building envelope components. Renewable Sustainable Energy Rev. 2011;15:3617-3631.

[22] Kamal MA. An overview of passive cooling techniques in buildings: Design concepts and architectural interventions. Acta Technica Napocensis: Civil Engineering & Architecture. 2012;50-1:84-97.

[23] Al-Obaidi KM, Ismail M, Rahman AMA. Passive cooling techniques through reflective and radiative roofs in tropical houses in Southeast Asia: A literature review. Frontiers of Architectural Research. 2014;3:283-297.

[24] Galiano A, Patania F, Nocera F, Galesi A. Performance assessment of a solar assisted desiccant cooling system. Therm. Sci. 2014;18:563-576.

[25] ⟨https://www.architecture.com/Explore/ArchitecturalStyles/Modernism.aspx⟩ Duncan J. Royal Institute of British Architects (RIBA). Architectural style: Modernism. 2016. [Visited 31.10.2016].

[26] Taleb HM. Using passive cooling strategies to improve thermal performance and reduce energy consumption of residential buildings in U.A.E. buildings. Frontiers of Architectural Research. 2014;3:154-165.

[27] Liu M, Wittchen KB, Heiselberg PK. Control strategies for intelligent glazed façade and their influence on energy and comfort performance of office buildings in Denmark. Appl. Energy. 2015;145:43-51.

[28] Caetano I, Santos L, Leitao A. From idea to shape, from algorithm to design: A framework for generation of contemporary facades. 16th International Conference, CAAD Futures 2015. Sao Paulo, Brazil: Springer; 2015.

[29] Nikpour M, Zin Kandar M, Ghasemi M, Ghomeshi M, Reza Safizadeh M. Heat transfer reduction using self shading strategy in energy comission building in Malaysia. J. Appl. Sci. 2012;12:897-901.

[30] Capeluto IG. Energy performance of the self-shading building envelope. Energy Build. 2003;35:327-36.

[31] Zerefos SC, Tessas CA, Kotsiopoulos AM, Founda D, Kokkini A. The role of building form in energy consumption: The case of a prismatic building in Athens. Energy Build. 2012;48:97-102.

[32] Chan ALS, Chow TT. Thermal performance of air-conditioned office buildings constructed with inclined walls in different climates in China. Appl. Energy. 2014;114:45-57.

[33] Rungta S. Design guide: Horizontal shading devices and light shelves; 2011. ⟨http://www.public.asu.edu/~kroel/www558/Shaily%20Vipul%20Assignment%203.pdf⟩.

[34] ⟨http://www.wbdg.org/resources/suncontrol.php⟩ Prowler D. Sun control and shading devices. National Institute of Building Sciences (NIBS); 2015. [Visited 31.10.2016].

[35] Atzeri A, Cappelletti F, Gasparella A, Shen H, Tzempelikos A. Assessment of long-term visual and thermal comfort and energy performance in open-space offices with different shading devices. 3rd International High Performance Buildings Conference at Purdue. United States: Purdue e-Pubs; 2014.

[36] Freewan AAY. Impact of external shading devices on thermal and daylighting performance of offices in hot climate regions. Sol. Energy. 2014;102:14-30.

[37] Al-Tamimi NA, Fadzil SFS. The potential of shading devices for temperature reduction in high-rise residential buildings in the Tropics. Procedia Eng. 2011;21:273-82.

[38] ⟨http://tboake.com/carbon-aia/strategies1b.html⟩ Reduce loads / demand first - shading (heat avoidance) The American Institute of Architects (AIA). Carbon neutral design (CND). Society of Building Science Educators (SBSE); 2012. [Visited 31.10.2016].

[39] Meyer U. Architectural guide Taiwan. DOM Publishers, Berlin, 2012.

[40] Lechner N. Heating, cooling, lighting: design methods for architects. Wiley, New York, 2001.

[41] ⟨http://www.wbdg.org/references/mou_daylight.php⟩ Ryan JT. Whole building design guide: Daylighting. National Institute of Building Sciences (NIBS); 2015. [Visited 31.10.2016].

[42] ⟨http://wiki.naturalfrequency.com/wiki/Solar_position⟩ Marsh A. Solar position. Natural Frequency; 2012. [Visited 31.10.2016].

[43] Szokolay SV. Solar Geometry. Passive and Low Energy Architecture International, The University of Queensland, Brisbane, 2007.

[44] ⟨http://www.new-learn.info/packages/clear/thermal/buildings/passive_system/solor_acess_control/external_shading.html⟩ Low Energy Architecture Research Unit (LEARN). External shading devices. Clear; 2015. [Visited 31.10.2016].

[45] ⟨http://www.slideshare.net/sbd09/sun-shade-calculator-for-lahore⟩ Khan S. Sun shade calculator. Edge Hill University; 2009. [Visited 31.10.2016].

[46] Marsh A. Computer-optimised shading devices. 8th International IBPSA Conference. Eindhoven, Netherlands: Building Simulation; 2003.

[47] Valladares-Rendón LG, Lo SL. Passive shading strategies to reduce outdoor insolation and indoor cooling loads by using overhang devices on a building. Build. Simul. 2014;7:671-81.

[48] Cho J, Yoo C, Kim Y. Viability of exterior shading devices for high-rise residential buildings: Case study for cooling energy saving and economic feasibility analysis. Energy Build. 2014;82:771-85.

[49] Chua KJ, Chou SK. Evaluating the performance of shading devices and glazing types to promote energy efficiency of residential buildings. Build. Simul. 2010;3:181-94.

[50] Kim G, Lim HS, Lim TS, Schaefer L, Kim JT. Comparative advantage of an exterior shading device in thermal performance for residential buildings. Energy Build. 2012;46:105-11.

[51] ⟨http://www.greengaragedetroit.com/index.php?title=Sustainable_Window_Design⟩ Brennan T, Brennan P. Sustainable window design. Green Garage; 2009. [Visited 31.10.2016].

[52] National Research Council Canada (NRCC). Adaptation guidelines for the national energy code of Canada for buildings 2011. Governemnt of Canada; 2011. ⟨http://www.nrc-cnrc.gc.ca/obj/doc/solutions-solutions/advisory-consultatifs/codes_centre-centre_codes/NECB_Adaptation_Guidelines.pdf⟩.

[53] ⟨https://courses.cit.cornell.edu/arch262/notes/03a.html⟩. Ochshorn A. Exterior wall requirements. Cornell University (CU); 2015. [Visited 31.10.2016].

[54] ⟨http://sustainabilityworkshop.autodesk.com/buildings/aperture-placement-area⟩ Walker J. Aperture placement and area. Autodesk Sustainability Workshop; 2011. [Visited 31.10.2016].

[55] Inanici MN, Demirbilek FN. Thermal performance optimization of building aspect ratio and south window size in five cities having different climatic characteristics of Turkey. Build. Environ. 2000;35:41-52.

[56] Yang Y, Li B, Yao R. All year heating and cooling load analysis for small hotel buildings in Guiyang city China. 10th Conference of the International Building Performance Simulation Association. Beijing, China: Proceeding of Building Simulation; 2007.

[57] Pino A, Bustamante W, Escobar R, Pino FE. Thermal and lighting behavior of office buildings in Santiago of Chile. Energy Build. 2012;47:441-9.

[58] Grynning S, Time B, Matusiak B. Solar shading control strategies in cold climates - heating, cooling demand and daylight availability in office spaces. Sol. Energy. 2014;107:182-94.

[59] Straube J. BSD-200: Low-energy commercial and institutional buildings: Top ten smart things to do for cold climates. Building Science Corporation (BSC); 2014. ⟨http://buildingscience.com/file/5321/download?token=Pmk2wN9i⟩.

[60] Erdim A, Manioğlu G. Building form effects on energy efficient heat pump application for different climatic zones. Faculty Arch. ITU A|Z. 2014;11:335-349.

[61] Correia-Guedes Sustainagle Architecture in Africa, in: Sayigh A. (Ed.), Sustainability, energy and architecture: Case studies in realizing green buildings, Elsevier Inc., Oxford, 2014, pp. 432–444.

[62] ⟨http://www.harvestenergysolutions.com/products/solar/siting⟩ Olinyk M, Curry C. Siting of photovoltaic panels. Harvest Solutions; 2015. [Visited 31.10.2016].

[63] Hii DJC, H CK, Lai-Choo ML, Zhang J, Ibrahim N, Huang YC, Janssen P. Solar radiation performance evaluation for high density urban forms in the tropical context. 12th Conference of International Building Performance Simulation Association. Sidney, Australia: Proceeding of Building Simulation; 2011.

[64] ⟨http://www.build.com.au/window-orientation-and-placement⟩ Connection Magazines. Window orientation and placement. Build; 2016. [Visited 31.10.2016].

[65] ⟨http://www.apricus.com/html/solar_collector_technical_info.htm#.WC7QIo996Uk⟩ Humphreys M. Collector installation guide. Apricus; 2016. [Visited 31.10.2016].

[66] ⟨http://www.heliodons.org/⟩ Lechner N. Heliodons. Helping to create a more sustainable future; 2015. [Visited 31.10.2016].

[67] Prinsloo G, Dobson R. Solar tracking. Stellenbosch University: SolarBooks. South Africa, 2015.

[68] Al-Anzi A, Khattab O. Solar conscious house design in Kuwait. J. Sci. Eng. 2010;37:59-72.

[69] Odunfa KM, Ojo TO, Odunfa VO, Ohunakin OS. Energy efficiency in building: Case of buildings at the University of Ibadan, Nigeria. J. Build. Constr. Plann. Res. 2015;03:18-26.

[70] Koranteng C, Abaitey EG. Simulation based analysis on the effects of orientation on energy performance of residential buildings in Ghana. J. Sci. Technol. 2009;29:86-101.

[71] Chan ALS. Effect of adjacent shading on the thermal performance of residential buildings in a subtropical region. Appl. Energy. 2012;92:516-22.

[72] Nurse P. Resilience to extreme weather: Sample of literature reviewed for chapter 3-defensive options. The Royal Society. 2014: 26-29

[73] Ralegaonkar RV, Gupta Rajiv. Review of intelligent building construction: A passive solar architecture approach. Renewable Sustainable Energy Rev. 2010;14:2238-2242.

[74] Kottek M, Grieser J, Beck C, Rudolf B, Rubel F. World map of Köppen-Geigen climate classification. Meteorol. Z. 2006;15: 259-263.

[75] Husain M. Consice geography: Climatology. Tata McGraw-Hill's. New Delhi, 2009, chapter2, pp. 28–36.

[76] ⟨http://www.tboake.com/carbon-aia/strategies1d.html⟩ Reduce loads / demand first - passive cooling. The American Institute of Architects (AIA). Carbon neutral design (CND). Society of Building Science Educators (SBSE); 2012. [Visited 31.10.2016].

[77] Chia SL, Ahmad MH, Ossen DR. The effect of geometric shape and building orientation on minimising solar insolation on high-rise buildings in hot humid climate. Journal of Construction in Developing Countries. 2007;12:27-38.

[78] ⟨http://www.level.org.nz/passive-design/location-orientation-and-layout/⟩ LEVEL. Passive design: Location, orientation, layout. 2016. [Visited 31.10.2016].

[79] Nayak JK, Prajapati JA. Indian Institute of Technology, Bombay and Solar Energy Centre, Ministry of non-conventional Energy Sources. Handbook on energy conscious buildings: Design guidelines. Government of india; 2006. ⟨http://mnre.gov.in/solar-energy/ch5.pdf⟩

[80] Reardon C, Downton P. Australian's guide to environmentally sustainable homes. Passive design: Design for climate. Australian Government; 2013. ⟨http://www.yourhome.gov.au/passive-design/design-climate⟩.

[81] Yang L, He BJ, Ye M. Application research of ECOTECT in residential estate planning. Energy Build. 2014;72:195-202.

[82] ⟨http://ecotect.com/v5-licence-management⟩ Marsh A. Autodesk® EcotectTM v5.6 licence managment. Autodesk, Inc; 2008. [Visited 06.11.2016].

[83] ⟨https://energyplus.net/weather⟩ U.S Department of Energy. EnergyPlus (DOE). Weather data. Building Technologies Office (BTO); 2016. [Visited 31.10.2016].

[84] Jentsch MF, Bahaj AS, James PAB. Climate change future proofing of buildings—Generation and assessment of building simulation weather files. Energy Build. 2008;40:2148-2168.

[85] Chronis A, Liapi KA, Sibetheros I. A parametric approach to the bioclimatic design of large scale projects: The case of a student housing complex. Energy Build. 2012;22:24-35.

[86] ⟨https://greendwell.wordpress.com/2009/09/18/climate-analysis-using-weather-tool-02/⟩ Greedwell. Climate Analysis using Weather Tool–02. WordPress; 2009. [Visited 31.10.2016].

[87] ⟨http://wiki.naturalfrequency.com/wiki/Optimum_Orientation⟩ Ecotect Community WIKI. Climate: Optimum orientation . Natural Frecuency 2016. [Visited 31.10.2016].

[88] ⟨http://www.yourhome.gov.au/passive-design/orientation⟩ McGee C. Australian's guide to environmentally sustainable homes. Australian Government; 2013. [Visited 31.10.2016].

[89] Morrissey J, Moore T, Horne RE. Affordable passive solar design in a temperate climate: An experiment in residential building orientation. Renewable Energy. 2011;36:568-577.

[90] Hornbachner D. Façade shading system. 3S Swiss Solar Systems AG; 2016. ⟨http://talev.fr/photovoltaique/facade/3SFACADE.pdf⟩.

[91] ⟨http://www.solarbuildingtech.com/High-Rise_Building_Solar_Remodeling/high_rise_building_solar_PV_remodeling_.htm⟩ Solar Building Tech. Solar PV Remodel High-rise Solar Building. Linvents Future Development; 2016. [Visited 31.10.2016].

[92] ⟨http://www.solar-constructions.com/wordpress/transparent-solar-panels/⟩ Porticer Solarteam. Transparent solar panels. Solar Constructions; 2016. [Visited 31.10.2016].

List of figures

Fig. 11 Elevation in 2D view of the annual insolation based on peak summer and winter months in Hong Kong [82].

Fig. 12 Top 2D view of the stereographic diagram with the *AZM* angles found for OBOSP and OBOSC in Hong Kong [82].

Fig. 13 *AZM* angles for OBOSP and ideal orientation worldwide: a) E orientation, b) NE orientation, c) W orientation and d) SE orientation.

Fig. 14 *AZM* angles for OBOSC and ideal orientation worldwide: a) S orientation, b) SE orientation, c) N orientation, d) NE orientation and e) NW orientation.

List of tables

Table 1 Angles for sizing overhangs on S-facing façades of the Northern Hemisphere according the Earth's latitude [40][41].

$L°$	24	25	26	27	28	29	30	31	32	33	34	35	36	37	38	39	40	41	42	43	44	45
$X°$	74	73	72	71	70	69	68	67	65.5	64.5	63.5	62.5	60.5	59.5	59	58.5	58	57	56	55	54	53
$Y°$	46	45	44	43	42	41	40	39	37.5	37.5	35.5	34.5	32.5	31.5	31	30.5	30	29	28	27	26	25

Table 2 Summary of EDR and PES achieved by the passive cases.

Class	Ref.	Country and city	Cli-mate	Base cases	Area	Method	Period	Passive strategy		Passive cases	
								Design	Type	EDR	PES
Façade self-shading (FSS)	[30]	Israel, Jerusalem	Csa	Mid-rise office prismatic building total 7-storey	49.6 m^2/ floor	Modelling SustArc, Simulation Energy	Annual	Simple	Mixed	0.64 kWh/m^2/y	43%
	[31]	Greece, Athens	Csa	Low-rise office semi-prismatic building total 2-storey	N.A	Simulation Energy, WinAir	Annual	Simple	Single	40.8 kWh/y	4.64%
	[32]	China, Hong Kong	Cwa	Low-rise office prismatic building total 1-storey	2304 m^2/ floor	Simulation EnergyPlus	Annual	Simple	Single	7.51 kWh/m^2/y	10.95%
Shading devices (SDs)	[47]	Taiwan, Taipei	Cfa	High-rise office rectangular building total 18-storey	1325 m^2/ floor	Modelling Revit, Simulation Ecotect	Annual	Simple	Single	16.73 kWh/m^2/y	8.92%
	[48]	South Korea, Seoul	Dwa	Mid-rise residential rectangular building total 8 units per floor	150 m^2/ S-unit	Simulation Ecotect, DaySim, DOE-2.1E	May-Sept	Simple	Single	14.81 kWh/m^2	19.70%
	[49]	Singapore, Singapore	Af	High-rise residential rectangular building total 20-storey	628 m^2/ floor	Simulation eQUEST	Annual	Simple	Single	N.A	7.20%
	[50]	South Korea, Seoul	Dwa	High-rise residential rectangular total 20-storey	145 m^2/ unit	Simulation IES_VE, Radiance, CFD	Annual	Complex	Single	22.68 kWh/m^2/y	66%
Window wall ratio (WWR)	[55]	Turkey, Antalya	Csa	Low-rise residential square building total 3-storey	200 m^2/ 2-unit	Simulation SUNCODE-PC	Annual	Simple	Single	36.11 kWh/m^2/y	54.17%
	[56]	China, Guiyang	Cwa	Low-rise hotel square building total 3-storey	N.A	Simulation DeST	Annual	Simple	Single	114,429 kWh/y	53.98%
	[57]	Chile, Santiago	BSk	Mid-rise office square building total 10-storey	256 m^2/ floor	Modelling Ecotect, Simulation, DaySim, Radiance	Annual	Simple	Mixed	82.4 kWh/m^2/y	76.57%
	[58]	Norway, Oslo	Dfc	Low-rise office square single-person cubicle total 1-storey	10.5 m^2/ S-unit	COMFEN, Simulation EnergyPlus	Annual	Simple	Mixed	52 kWh/m^2/y	27.95%
Building orientation (BO)	[68]	Kuwait City, Kuwait	BWh	Low-rise residential hexagonal house total 2-storey	707 m^2/ floor	Simulation VisualDOE	Aug.	Complex	Mixed	0.05 kWh/m^2	43%
	[69]	Nigeria, Ibadan	Aw	Low-rise institutional square building total 2-storey	N.A	CLTD/CLF method	Annual	Simple	Single	7.96 kWh/y	4.87%
	[70]	Ghana, Bohyen	Aw	Low-rise residential rectangular building total 1-storey	137 m^2/ floor	Simulation EDSL 2008	Annual	Simple	Single	1.57 kWh/m^2/y	16.02%
	[71]	China, Hong Kong	Cwa	High-rise residential rectangular building total 40-storey	30,400 m^2/ block	Simulation EnergyPlus Shadow Algorithm	Annual	Simple	Single	11.18 kWh/m^2/y	19.76%

Table 3 Strategy types classified by the PES and categorised by its parameters.

Ref	Class	Zone	Cli-mate	Strategy type by PES		Strategy type by parameters							
						wall geometry		wall size		shading design			glazing ratio
				single %	mixed %	shape	$\hat{Z}$, $\tilde{V}$ angles	length large	length short	position alignment	*VSA* angles	place-ment	aperture %
[55]	WWR	SUBT	Csa	54.17	-	square	all 90°	-	-	-	-		25
[56]	WWR	SUBT	Cwa	53.98	-	square	all 90°	-	-	-	-		25
[57]	WWR	SUBT	BSk	-	76.57	square	all 90°	-	-	horizontal internal blinds	- -	N E,W	20
[58]	WWR	TEMP	Dfc	-	27.95	square	all 90°	-	-	-	-		41
[47]	SDs	SUBT	Cfa	8.92	-	rectangular	all 90°	–	–	horizontal	-	N,S, E,W	-
[48]	SDs	TEMP	Dwa	19.70	-	rectangular	all 90°	–	–	horizontal	-	S	-
[49]	SDs	TROP	Af	7.20	-	rectangular	all 90°	–	–	overhang tilt	30°	W	-
[50]	SDs	TEMP	Dwa	66.00	-	rectangular	all 90°	–	–	overhang tilt slats tilt	- 60°	- S	-
[68]	BO	SUBT	BWh	-	43.00	hexagonal	all 90°	N-S	E-W	horizontal internal blinds open buffer zones	- -	N S E, W	-
[69]	BO	TROP	Aw	4.87	-	rectangular	all 90°	N-S	E-W	-	-		-
[70]	BO	TROP	Aw	16.02	-	rectangular	all 90°	N-S	E-W	-	-		-
[71]	BO	SUBT	Cwa	19.76	-	rectangular	all 90°	N-S	E-W	-	-		-
[30]	FSS	SUBT	Csa	-	43.00	prismatic	S-31° W-34° E-34°	-	-	internal blinds	-	W	-
[31]	FSS	SUBT	Csa	4.64	-	semi-prismatic	S-143° W-7° E-4°	-	-	-	-	-	-
[32]	FSS	SUBT	Cwa	10.95	-	prismatic	all 40°	-	-	-	-	-	-

Table 4 Worldwide guide of *AZM* angles found for OBOSP and OBOSC [74][83].

Climate	Type	Hemi-sphere	Location		Country	City	*AZM* angles			
			latitude	longitude			OBOSP overheated short façade		OBOSC underheated large façade	
Af	tropical rainforest no summer no winter	NH	3.10	101.70	Malaysia	Kuala Lumpur	127.5°	SE	37.5°	NE
		NH	1.40	104.0	Singapore	Singapore	75.0°	NE	165.0°	SE
		NH	26.70	-80.10	United States	W. Palm Beach	87.5°	E	177.5°	S
		SH	-7.20	112.70	Indonesia	Surabaya	-	-	-	-
Am	tropical monsoon large rainy season short dry season	NH	25.70	-80.20	United States	Miami	260.0°	W	170.0°	S
		SH	-6.10	106.70	Indonesia	Jakarta	-	-	-	-
		NH	16.00	108.20	Vietnam	Da Nang	-	-	-	-
		SH	-5.10	119.40	Indonesia	Makassar	-	-	-	-
Aw	tropical savanna summer wet season winter dry season	SH	-15.90	-47.90	Brazil	Brasilia	57.5°	NE	327.5°	NW
		NH	19.10	72.80	India	Mumbai	107.5°	SE	17.5°	NE
		SH	-22.90	-43.20	Brazil	Rio de Janeiro	-	-	-	-
		NH	110.70	106.70	Vietnam	Ho Chi Minh	-	-	-	-
BWh	arid desert hot	NH	30.10	31.40	Egypt	Cairo	95.0°	E	185.0°	S
		NH	124.60	46.70	Saudi Arabia	Riyadh	82.5°	E	172.5°	S
		SH	-12.00	-77.10	Peru	Lima	70.0°	NE	340.0°	NW
		NH	29.2	48	Kuwait	Kuwait	90.0°	E	180.0°	S
BWk	arid desert cold	NH	35.30	-113.90	United States	Kingman	90.0°	E	180.0°	S
		SH	-23.40	-70.40	Chile	Antofagasta	95.0°	E	5.0°	N
		SH	-26.60	15.10	Namibia	Lüderitz	-	-	-	-
		SH	-32.88	-68.81	Argentina	Mendoza	-	-	-	-
BSh	semi-arid steppe hot	NH	28.50	77.20	India	New Delhi	100.0°	E	190.0°	S
		SH	-23.30	43.60	Madagascar	Tulear	-	-	-	-
BSk	semi-arid steppe cold	SH	-33.40	-70.80	Chile	Santiago	85.0°	E	355.0°	N
		NH	50.70	-120.40	Canada	Kamloops	75.0°	NE	165.0°	SE
		NH	47.90	107.0	Mongolia	Ulaanbaatar	82.5°	E	172.5°	S
		NH	38.00	46.20	Iran	Tabriz	80.0°	E	170.0°	S
Csa	mediterranean dry summer hot summer	SH	-34.90	138.60	Australia	Adelaide	272.5°	W	2.5°	N
		NH	43.70	7.20	France	Nice	80.0°	E	170.0°	S
		NH	37.90	23.70	Greece	Athens	72.5°	NE	162.5°	SE
		NH	41.80	12.60	Italy	Rome	82.5°	E	172.5°	S
Csb	mediterranean dry summer warm summer	NH	49.20	-123.10	Canada	Vancouver	77.5°	E	167.5°	S
		NH	37.70	-122.40	United States	San Francisco	280.0°	W	190.0°	S
		NH	47.60	-122.30	United States	Seattle	275.0°	W	185.0°	S
		NH	44.90	-123.00	United States	Salem	-	-	-	-
Csc	maritime subalpine dry summer cold summer	SH	-38.85	-71.69	Chile	Melipeuco	-	-	-	-
		SH	-45.90	-71.70	Chile	Balmaceda	-	-	-	-
Cwa	temperate dry winter hot summer	NH	23.10	113.20	China	Hong Kong	282.5°	W	192.5°	S
		NH	21.00	105.80	Vietnam	Hanoi	52.5°	NE	322.5°	NW
Cwb	maritime temperate dry winter warm summer	NH	19.40	-99.10	Mexico	Mexico City	105.0°	E	15.0°	N
		NH	4.70	-74.10	Colombia	Bogota	152.5°	SE	62.5°	NE
		SH	-26.10	28.00	South Africa	Johannesburg	95.0°	E	5.0°	N
		SH	-15.49	-70.12	Peru	Juliaca	-	-	-	-
Cwc	maritime temperate dry winter cold summer	SH	-16.50	-68.20	Bolivia	La Paz	102.5°	E	12.5°	N
		SH	-16.16	-69.08	Bolivia	Copacabana	-	-	-	-
Cfa	temperate no dry season hot summer	NH	31.20	121.40	China	Shanghai	80.0°	E	170.0°	S
		NH	25.10	121.50	Taiwan	Taipei	85.0°	E	175.0°	S
		NH	40.70	-73.90	United States	New York	272.5°	W	182.5°	S
		NH	45.40	12.30	Italy	Venice	67.5°	NE	157.5°	SE
Cfb	maritime no dry season warm summer	NH	46.20	6.10	Switzerland	Geneva	85.0°	E	175.0°	S
		NH	48.10	11.50	Germany	Munich	75.0°	NE	165.0°	SE
		NH	51.40	0.0	United Kingdom	London	82.5°	E	172.5°	S
		NH	-41.30	174.80	New Zealand	Wellington	95.0°	E	5.0°	N

Cfc	maritime subarctic no dry season cold summer	NH	57.80	-152.30	Alaska	Kodiak	82.5°	E	172.5°	S
		NH	64.10	21.90	Iceland	Reykjavik	82.5°	E	172.5°	S
Dsa	continental dry summer hot summer									
Dsb	continental dry summer warm summer	NH	47.60	-117.50	United States	Spokane	80.0°	E	170.0°	S
		NH	41.50	-71.30	United States	Newport	-	-	-	-
Dsc	continental subarctic dry summer cold summer	NH	61.10	-150.00	Alaska	Anchorage	282.5°	W	192.5°	S
		NH	60.60	-151.20	Alaska	Kenai	82.5°	E	172.5°	S
Dsd	continental subarctic dry summer very cold winter									
Dwa	continental dry winter hot summer	NH	41.50	123.80	China	Fushun	82.5°	E	172.5°	S
		NH	37.50	126.90	Korea	Seoul	67.5°	NE	157.5°	SE
		NH	39.80	116.50	China	Beijing	85.0°	E	175.0°	S
		NH	45.70	126.60	China	Harbin	-	-	-	-
Dwb	continental subarctic dry winter warm summer	NH	43.10	131.9	Russia	Vladivostok	-	-	-	-
		NH	51.10	-114.00	Canada	Calgary	82.5°	E	172.5°	S
Dwc	continental subarctic dry winter cold summer	NH	50.42	124.07	China	Jiagedaqi	-	-	-	-
Dwd	continental dry winter very cold winter	NH	63.46	142.78	Russia	Oymyakon	-	-	-	-
Dfa	continental no dry season hot summer	NH	41.80	-87.80	United States	Chicago	82.5°	E	172.5°	S
		NH	44.50	26.10	Romania	Bucharest	85.0°	E	175.0°	S
		NH	42.30	-83.00	Canada	Windsor	80.0°	E	170.0°	S
		SH	-33.05	-71.60	Chile	Valparaiso	-	-	-	
Dfb	continental no dry season warm summer	NH	52.20	21.00	Poland	Warsaw	75.0°	NE	165.0°	SE
		NH	55.70	37.60	Russia	Moscow	65.0°	NE	155.0°	SE
		NH	59.90	30.30	Russia	St. Petersburg	72.5°	NE	162.5°	SE
		NH	50.10	14.30	Czech Republic	Prague	82.5°	E	172.5°	S
Dfc	continental subarctic no dry season cold summer	NH	45.40	-73.70	Canada	Montreal	75.0°	NE	165.0°	SE
		NH	43.60	-79.60	Canada	Toronto	67.5°	NE	157.5°	SE
		NH	64.80	-147.90	Alaska	Fairbanks	85.0°	E	175.0°	S
		NH	64.50	40.60	Russia	Archangelsk	-	-	-	
Dfd	continental subarctic no dry season very cold winter	NH	62.10	129.80	Russia	Yakutsk	85.0°	E	175.0°	S
		NH	62.93	152.38	Russia	Seymchan	-	-	-	
ETf	polar tundra no dry season	NH	71.30	-156.70	Alaska	Barrow	80.0°	E	170.0°	S
		NH	60.14	-45.24	Greenland	Nanortalik	-		-	
Climate 28			Locations 82		Countries 40	Cities 82	Simulations 59			

Table 5 Relationship between the *AZM* angle groups with their ideal orientations [2][88].

AZM angle group	346°~0°~15°	16°~75°	76°~90°~105°	106°~165°
Ideal orientation	N-oriented	NE-oriented	E-oriented	SE-oriented
AZM angle group	166°~180°~195°	196°~255°	256°~270°~285°	286°~345°
Ideal orientation	S-oriented	SW-oriented	W-oriented	NW-oriented